Measurement of heavy-flavor jet axes differences in pp collisions with ALICE

Hot Jets January 2025
University of Illinois Urbana-Champaign

By Emma Yeats
University of California Berkeley

On behalf of the ALICE Collaboration

Introduction to Heavy-Flavor

Heavy-flavor quarks produced in pp collisions allow us to investigate the evolution of quark-initiated parton showers – from the initial hard scatterings to final-state hadrons!

Jets tagged with a heavy quark provide insight into both perturbative and non-perturbative effects on jet formation and structure.

Introduction to Heavy-Flavor

Heavy-flavor quarks produced in pp collisions allow us to investigate the evolution of quark-initiated parton showers – from the initial hard scatterings to final-state hadrons!

Jets tagged with a heavy quark provide insight into both perturbative and non-perturbative effects on jet formation and structure.

Flavor effects include:

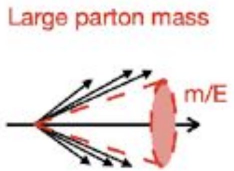

The dead-cone effect: gluon emissions are suppressed in a cone with $\theta = m_Q/E$.

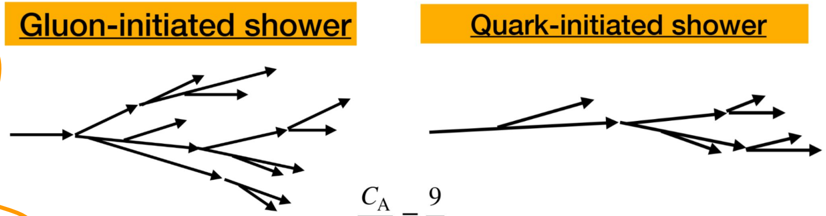

$$\frac{C_A}{C_F} = \frac{9}{4}$$

Casimir color factors: gluon-initiated showers are expected to have a broader and softer fragmentation profile than quark-initiated showers.

See P. Dhankher's Talk from Wed.

Introduction to Heavy-Flavor

Heavy-flavor quarks produced in pp collisions allow us to investigate the evolution of quark-initiated parton showers – from the initial hard scatterings to final-state hadrons!

Jets tagged with a heavy quark provide insight into both perturbative and non-perturbative effects on jet formation and structure.

See P. Dhankher's Talk from Wed.

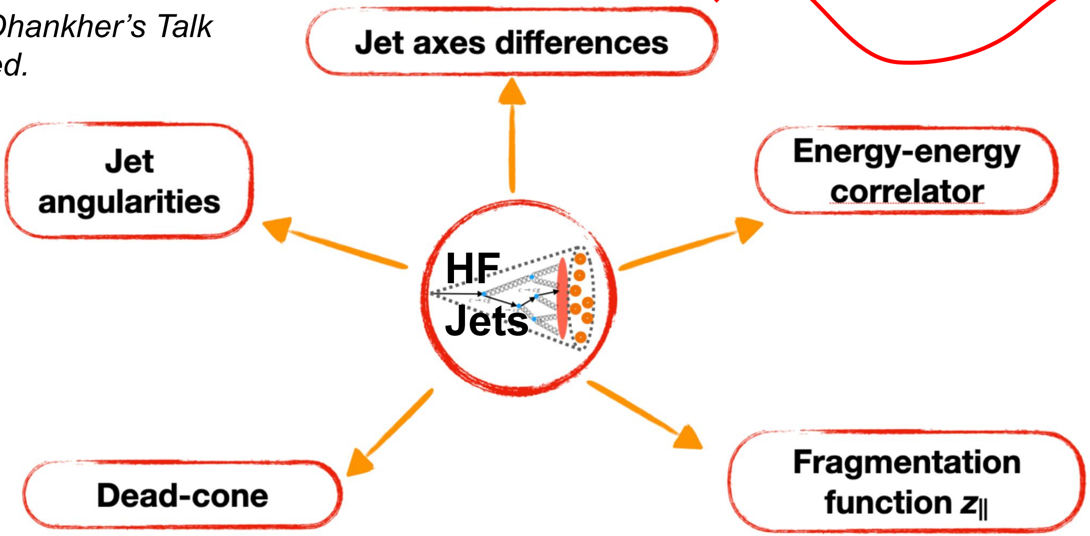

Jet axes differences

Jet angularities

Energy-energy correlator

HF Jets

Dead-cone

Fragmentation function $z_{\parallel}$

$$\Delta R = \sqrt{(\Delta y)^2 + (\Delta \phi)^2}$$

This talk discusses D^0-tagged *Jet Axes Differences (ΔR)*

(aka the angular difference between jet axes!)

Introduction to ΔR

Question: which jet axes to study?

← **sensitivity to soft radiation**

Jet Axes Definitions:

Standard (STD): The jet axis resulting from clustering the constituents of a jet containing a D^0 meson with anti-k_T algorithm, R=0.4

Soft Drop (groomed) (SD): Standard jet reclustered with Cambridge-Aachen with the *SD condition* applied to it:

$$\frac{min(p_{T_1}, p_{T_2})}{p_{T_1} + p_{T_2}} > z_{cut} \left(\frac{\Delta R_{12}}{R} \right)^{\beta}$$

$z_{cut}=0.1, \beta=0$

$z_{cut}=0.2, \beta=0$

Winner-Takes-All (WTA): Standard jet reclustered with Cambridge-Aachen algorithm and recombined using *WTA recombination* scheme.

Aligns the axis with the hardest subjet at each clustering step

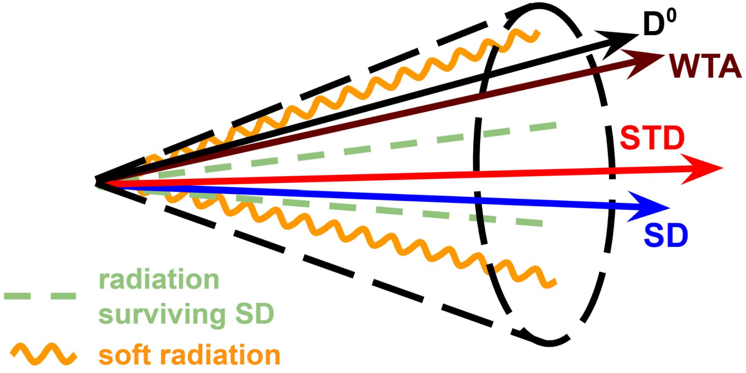

Introduction to *ΔR*

Jet Axes Difference (ΔR) is the angular difference between jet axes!

$$\Delta R = \sqrt{(\Delta y)^2 + (\Delta \phi)^2}$$

The angular openings between the three jet axes give us three combinations:

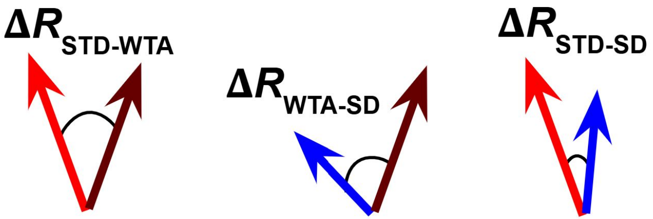

We can also study the angle between any jet axis and the direction of the D^0 meson

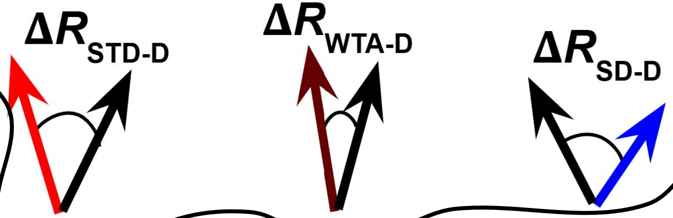

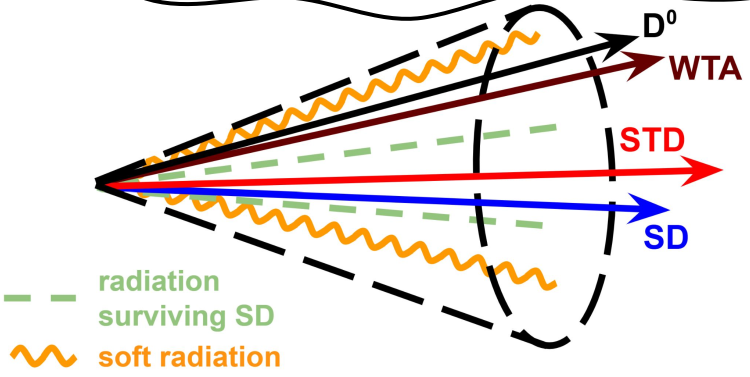

These six observables were measured in proton-proton collisions at √*s* = 5.02 TeV collected from the ALICE experiment at the LHC in Run 2.

Motivation

Why study ΔR for D^0-tagged jets?

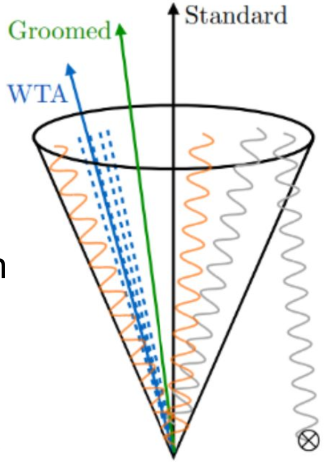

- ➔ Heavy-flavor quarks are effective probes to **test perturbative QCD** calculations in pp collisions, and ΔR is calculable perturbatively [Cal, Neill, Ringer, Waalewijn].
- ➔ ΔR has been studied for the inclusive sample of jets, but extending to HF-tagged jets will help us **understand flavor dependencies (dead-cone and color-charge effects) during the fragmentation process**.
- ➔ By studying these three different axes we are able to **tune our sensitivity to soft radiation**
  - ◆ by considering angles between different axes, we are sensitive to the **radiation pattern inside the reconstructed jets**.
  - ◆ angles between the heavy quark and a jet axis allows us to study the **flavor dependence of the fragmentation process** by comparing to inclusive-jet results.

P. Cal, D. Neill, F. Ringer, and W. J. Waalewijn, "Calculating the angle between jet axes," JHEP 04 (2020) 211, arXiv:1911.06840 [hep-ph].

Analysis Methods

**more details on the analysis methods in backup slides!*

For each jet axis difference observable…

1. D^0 candidates were reconstructed from daughter tracks using topological selections and particle identification on daughter tracks ($D^0 \rightarrow K^- + \pi^+$, and charge conjugate).

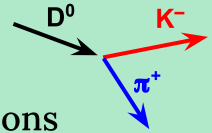

Analysis Methods

**more details on the analysis methods in backup slides!*

For each jet axis difference observable…

1. D^0 candidates were reconstructed from daughter tracks using topological selections and particle identification on daughter tracks ($D^0 \rightarrow K^- + \pi^+$, and charge conjugate).

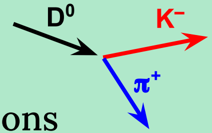

2. D^0-tagged charged jets reconstructed by implementing anti-k_T algorithm (R=0.4) separately for each D^0 candidate in an event.

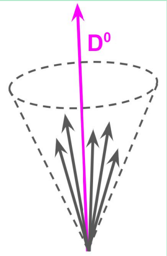

Analysis Methods

**more details on the analysis methods in backup slides!*

For each jet axis difference observable…

1. D^0 candidates were reconstructed from daughter tracks using topological selections and particle identification on daughter tracks ($D^0 \rightarrow K^- + \pi^+$, and charge conjugate).

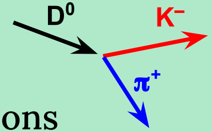

2. D^0-tagged charged jets reconstructed by implementing anti-k_T algorithm (R=0.4) separately for each D^0 candidate in an event.

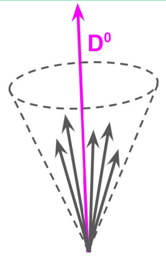

3. Invariant-mass sideband-subtraction technique removes the contribution of combinatorial $K^-\pi^+$ pairs surviving the D^0 selections from the ΔR distribution.

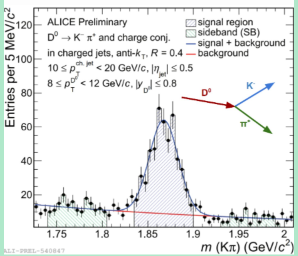

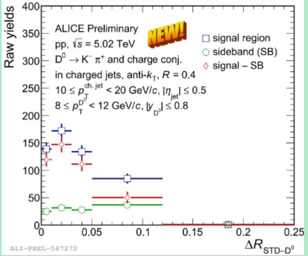

Analysis Methods

**more details on the analysis methods in backup slides!*

For each jet axis difference observable…

1. D^0 candidates were reconstructed from daughter tracks using topological selections and particle identification on daughter tracks ($D^0 \rightarrow K^- + \pi^+$, and charge conjugate).

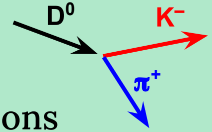

2. D^0-tagged charged jets reconstructed by implementing anti-k_T algorithm (R=0.4) separately for each D^0 candidate in an event.

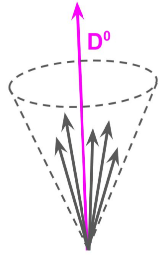

3. Invariant-mass sideband-subtraction technique removes the contribution of combinatorial $K^-\pi^+$ pairs surviving the D^0 selections from the ΔR distribution.

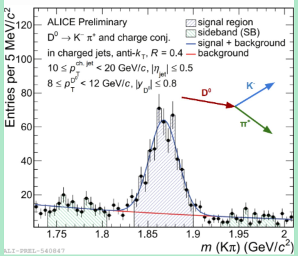

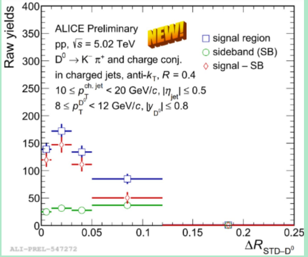

4. Corrected for the efficiency of D^0-tagged jet reconstruction and removed the contribution from beauty decays.

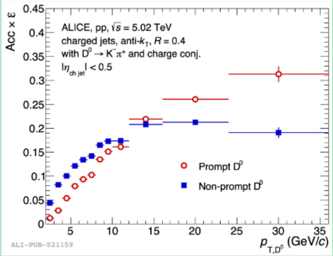

Analysis Methods

**more details on the analysis methods in backup slides!*

For each jet axis difference observable…

1. D^0 candidates were reconstructed from daughter tracks using topological selections and particle identification on daughter tracks ($D^0 \rightarrow K^- + \pi^+$, and charge conjugate).

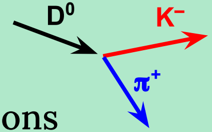

2. D^0-tagged charged jets reconstructed by implementing anti-k_T algorithm (R=0.4) separately for each D^0 candidate in an event.

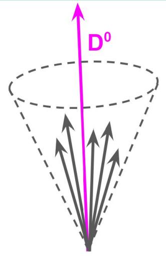

3. Invariant-mass sideband-subtraction technique removes the contribution of combinatorial $K^-\pi^+$ pairs surviving the D^0 selections from the ΔR distribution.

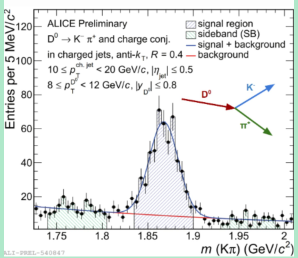

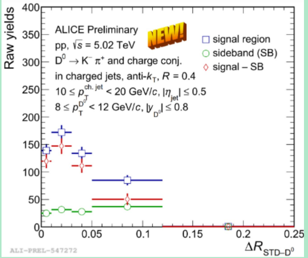

4. Corrected for the efficiency of D^0-tagged jet reconstruction and removed the contribution from beauty decays.

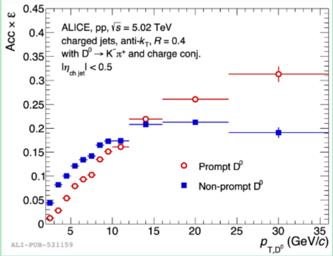

5. Corrected for detector effects with an iterative Bayesian unfolding approach.

Results: The Ungroomed Sample of Jets

$\Delta R_{\text{STD-D}}$

$\Delta R_{\text{WTA-D}}$

$\Delta R_{\text{STD-WTA}}$

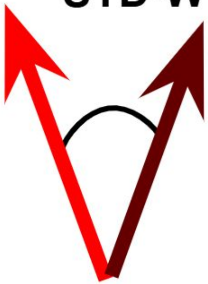

STD-D vs STD-WTA

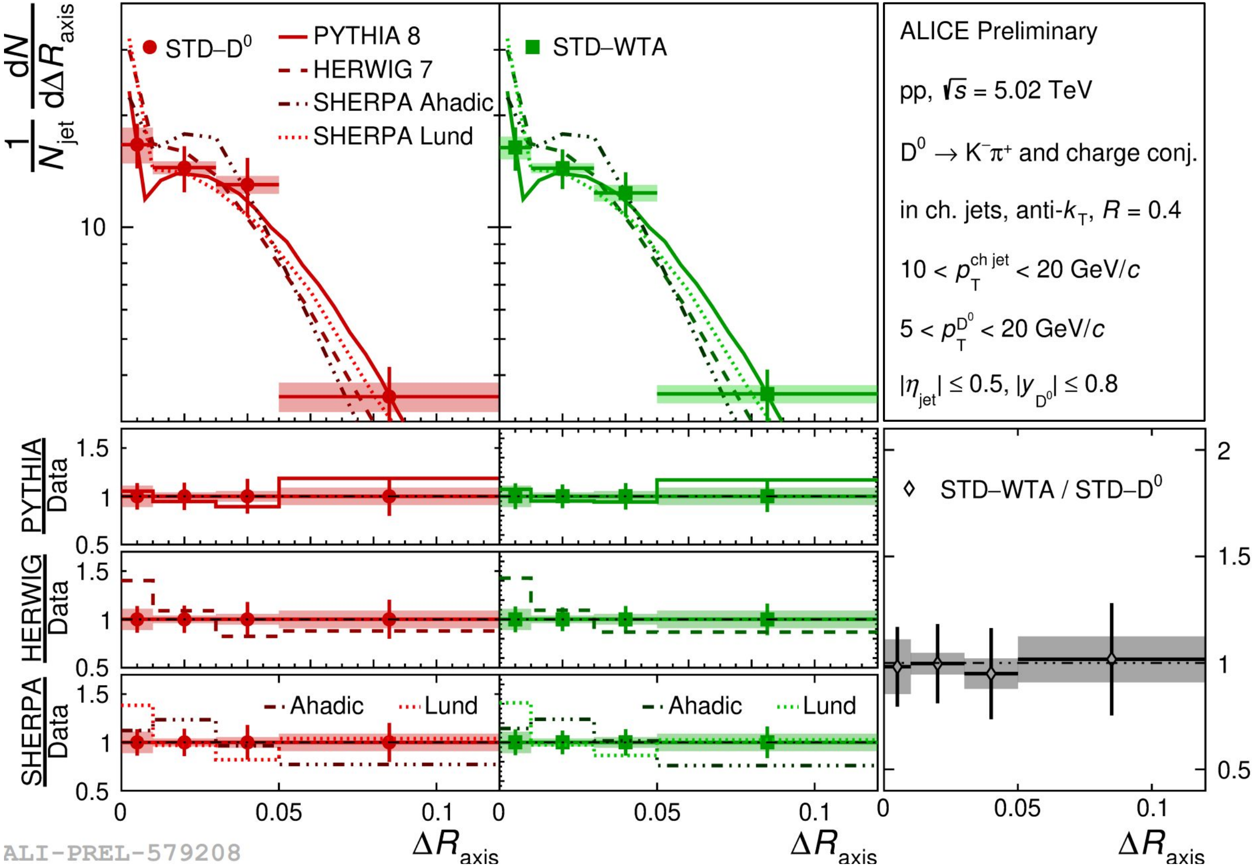

ALI-PREL-579208

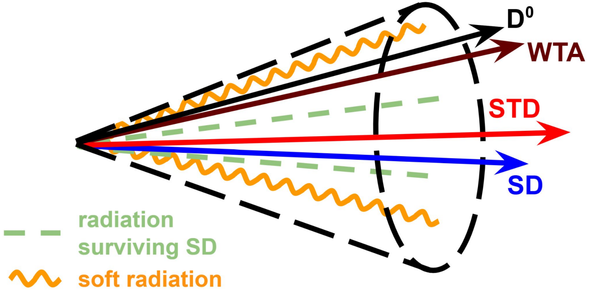

Three findings here:

STD-D vs STD-WTA

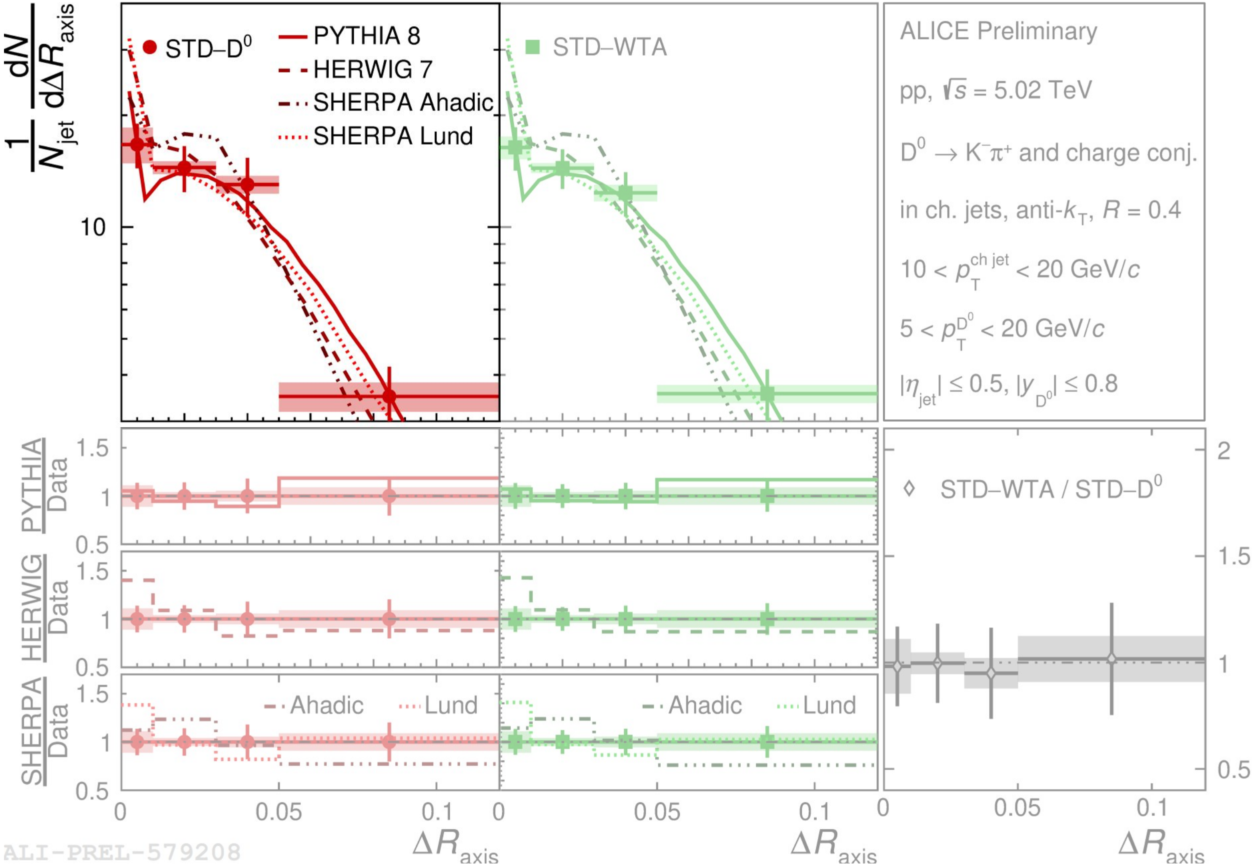

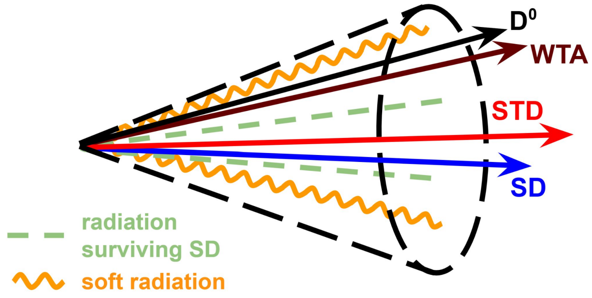

Three findings here:

#1: The D^0 does not define the Standard axis direction

STD-D vs STD-WTA

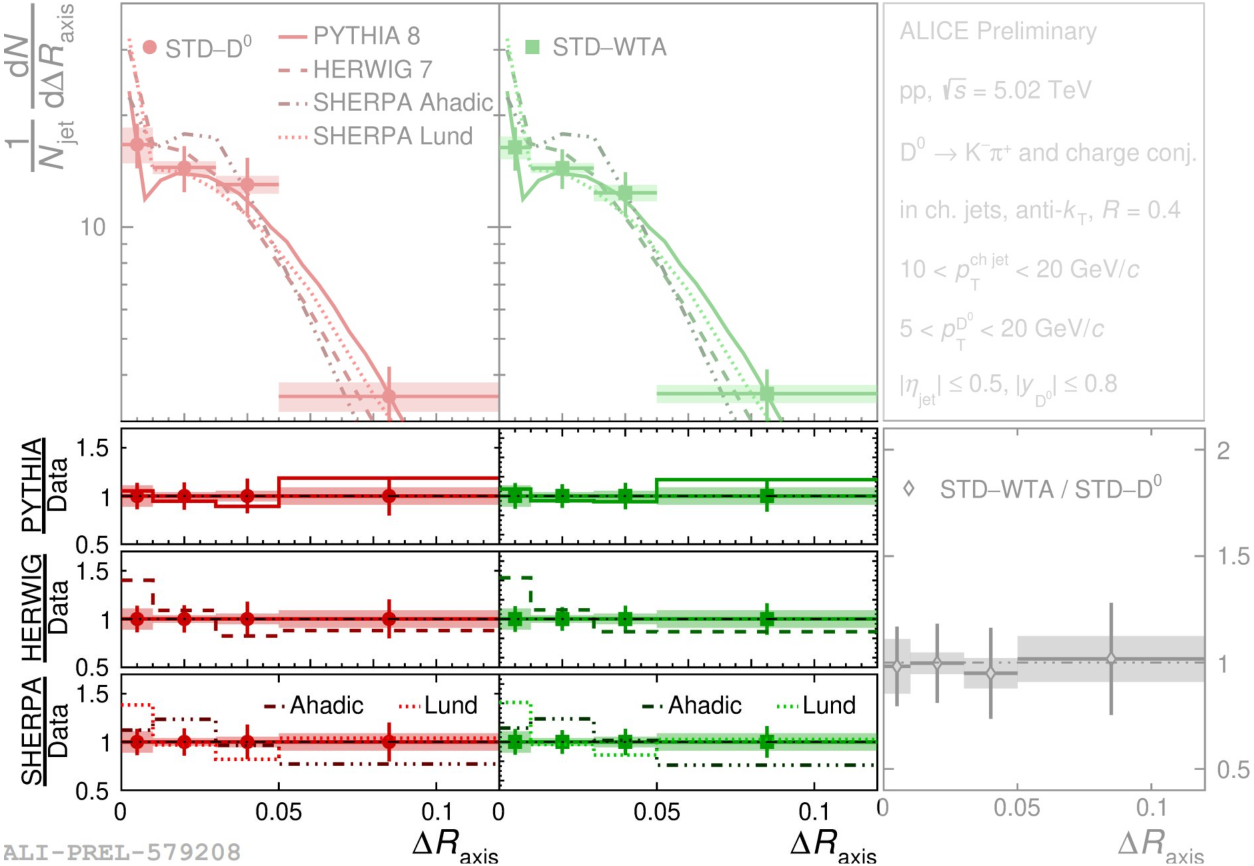

ALI-PREL-579208

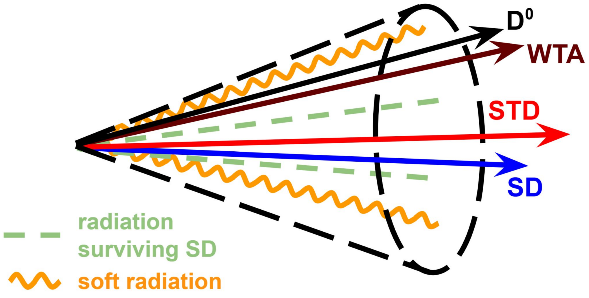

Three findings here:

#1: The D^0 does not define the Standard axis direction

#2: Lund-String based models predict the data best (PYTHIA performs well!)

STD-D vs STD-WTA

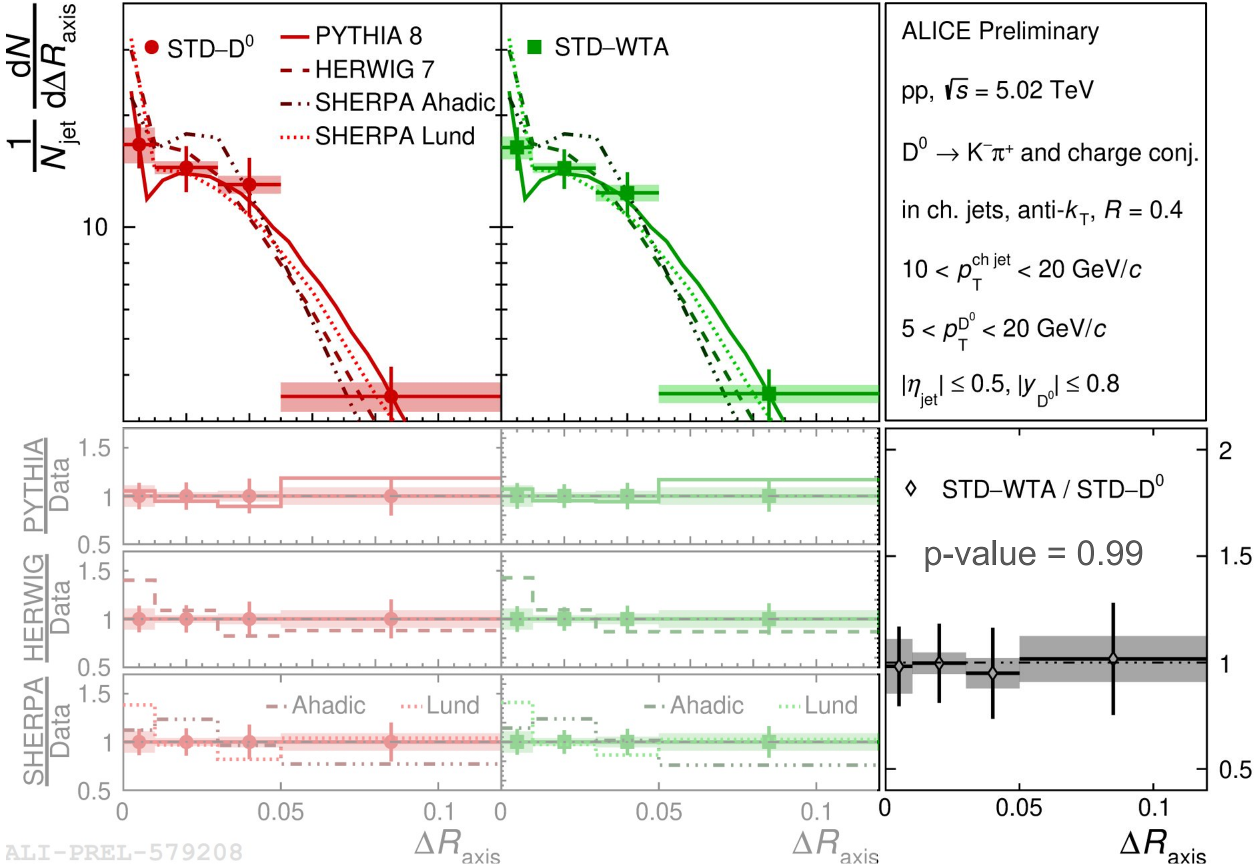

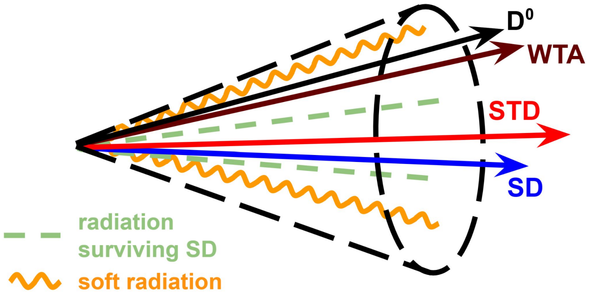

Three findings here:

#1: The D^0 does not define the Standard axis direction

#2: Lund-String based models predict the data best (PYTHIA performs well!)

#3: **STD-D** matches **STD-WTA**! Leads us to…

WTA-D

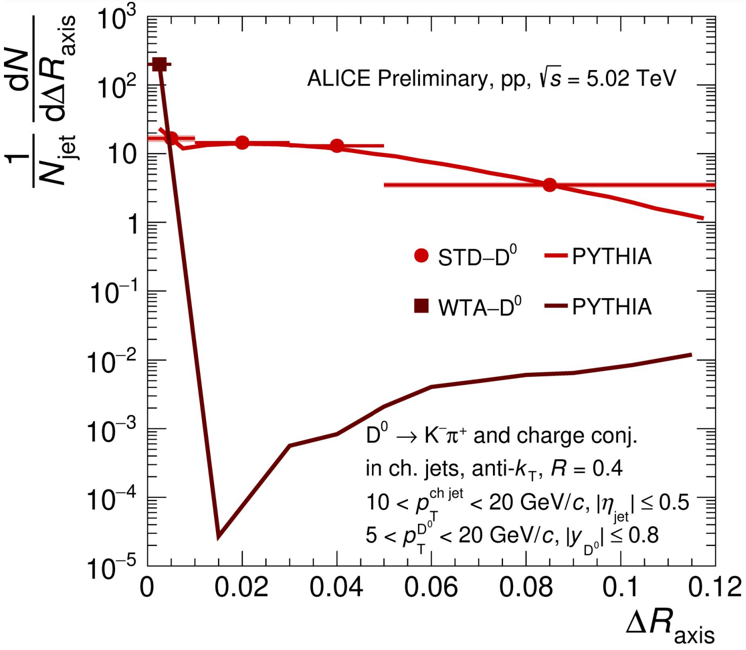

Extremely strong alignment is seen between the WTA and the D^0 direction

WTA-D

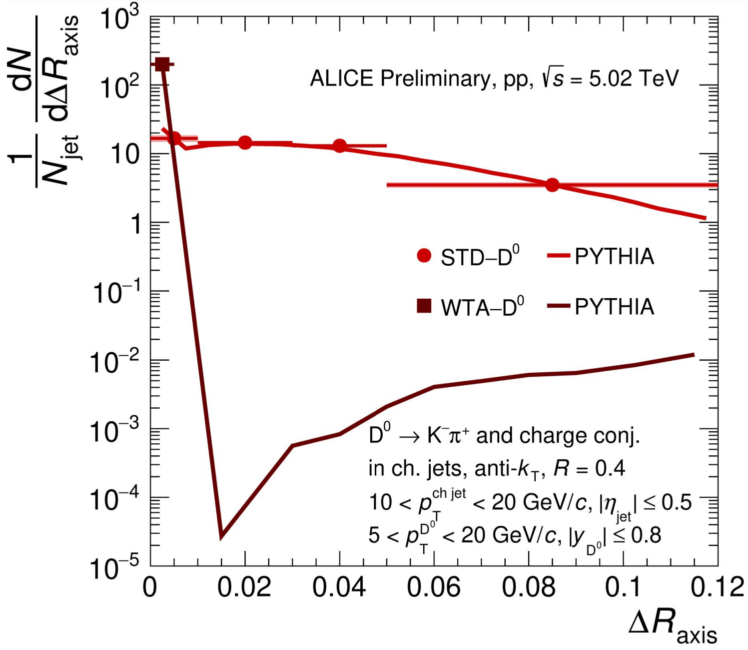

Fraction of jets in $0 < \Delta R < 0.005$ for $\Delta R_{\mathrm{WTA-D^0}}$

Distribution	$10 < p_{\mathrm{T,ch\ jet}} < 20$ GeV/c $5 < p_{\mathrm{T,D^0}} < 20$ GeV/c	$20 < p_{\mathrm{T,ch\ jet}} < 50$ GeV/c $12 < p_{\mathrm{T,D^0}} < 50$ GeV/c
Measurement	$99\% \pm 0.001\%$	$95\% \pm 2\%$
Systematics	$\pm 1\%$	$\pm 5\%$
PYTHIA8	$99\% \pm 0.01\%$	$99\% \pm 0.03\%$

Extremely strong alignment is seen between the WTA and the D^0 direction - in both jet p_T regions!

Result #3 (STD-D matches **STD-WTA)** can be summarized with a more fundamental statement:

WTA ≃ D!

WTA-D

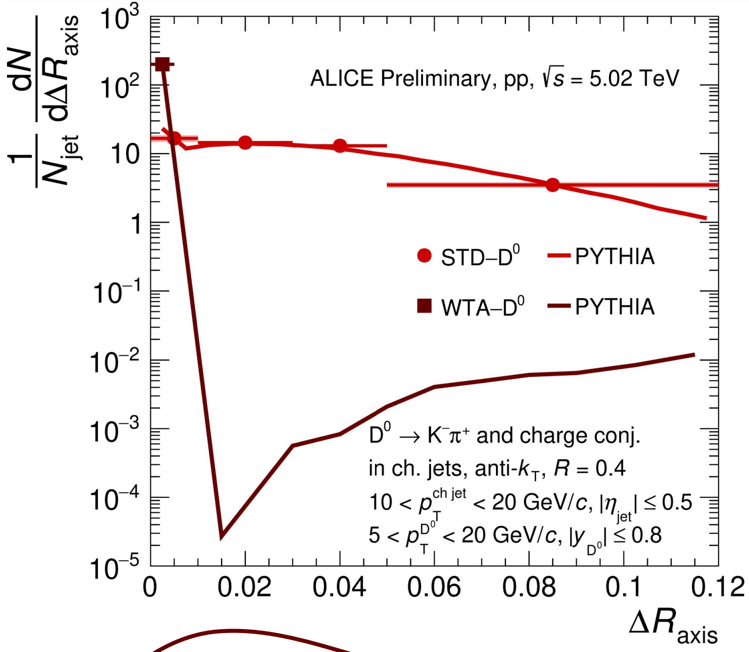

Fraction of jets in $0 < \Delta R < 0.005$ for $\Delta R_{\mathrm{WTA-D^0}}$

Distribution	$10 < p_{\mathrm{T,ch\ jet}} < 20$ GeV$/c$ $5 < p_{\mathrm{T,D^0}} < 20$ GeV$/c$	$20 < p_{\mathrm{T,ch\ jet}} < 50$ GeV$/c$ $12 < p_{\mathrm{T,D^0}} < 50$ GeV$/c$
Measurement	$99\% \pm 0.001\%$	$95\% \pm 2\%$
Systematics	$\pm 1\%$	$\pm 5\%$
PYTHIA8	$99\% \pm 0.01\%$	$99\% \pm 0.03\%$

Extremely strong alignment is seen between the WTA and the D^0 direction - in both jet p_T regions!

Result #3 (STD-D matches **STD-WTA)** can be summarized with a more fundamental statement:

WTA ≃ D!

WTA-D alignment implies the D^0 meson is the winner (in the hardest prong).

WTA scheme: at each recombination step, the resulting prong has the direction of the hardest sub-prong

Previous measurements of the fragmentation of charm jets showed that the D^0 is usually the leading particle, but this measurement of WTA-D clearly shows **how often** this is true (99% of the time).

https://arxiv.org/pdf/2204.10167

Results: The Groomed Sample of Jets

Before turning to our results, what do we expect to see?

Results: The Groomed Sample of Jets

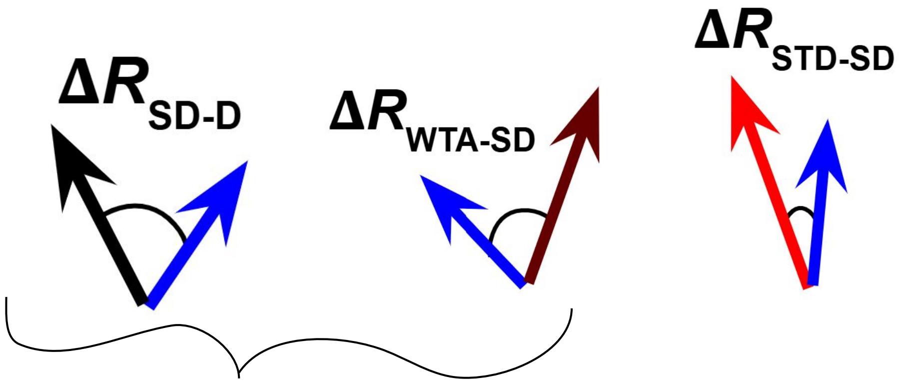

Before turning to our results, what do we expect to see?

Due to **WTA** ≃ **D**, we expect **SD-D** to match **WTA-SD**.

Indeed this is what we see, with a p-value=0.99 for both cases of z_{cut} (more detail in backup slides)

Since they are almost interchangeable, we will discuss **SD-D** only

Results: The Groomed Sample of Jets

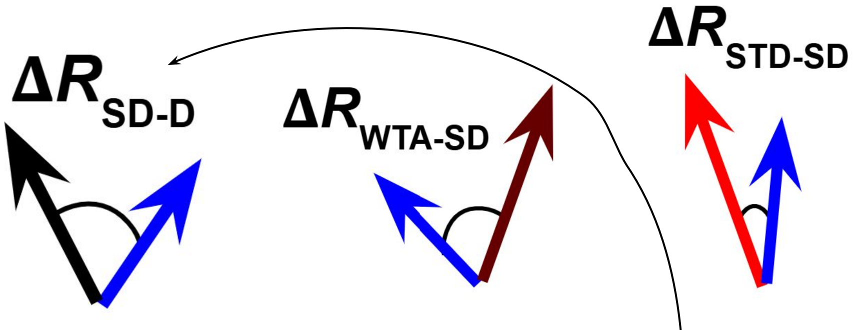

Before turning to our results, what do we expect to see?

SD-D shows how grooming (removing any radiation softer than z_{cut}) affects **STD-D**

Due to **WTA ≃ D**, we expect **SD-D** to match **WTA-SD**.

Indeed this is what we see, with a p-value=0.99 for both cases of z_{cut} (more detail in backup slides)

Since they are almost interchangeable, we will discuss **SD-D** only

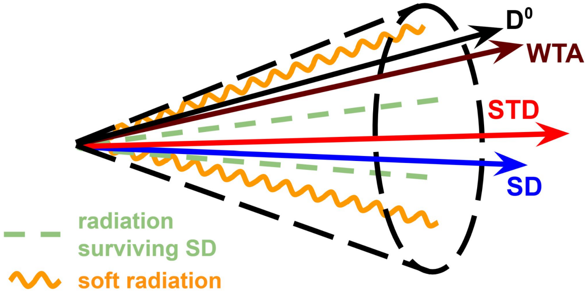

Results: The Groomed Sample of Jets

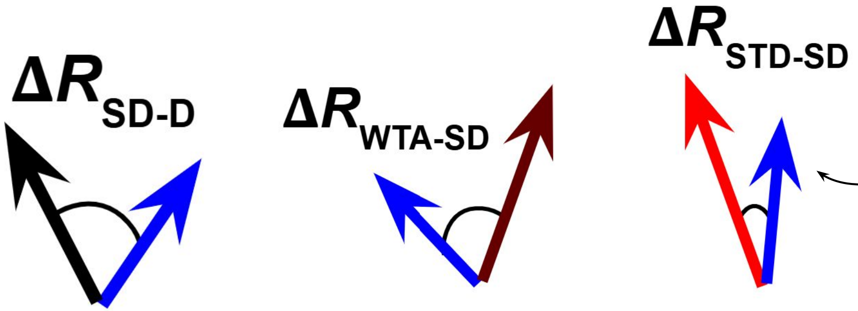

Before turning to our results, what do we expect to see?

Due to **WTA** ≃ **D**, we expect **SD-D** to match **WTA-SD**.

Indeed this is what we see, with a p-value=0.99 for both cases of z_{cut} (more detail in backup slides)

Since they are almost interchangeable, we will discuss **SD-D** only

SD-D shows how grooming (removing any radiation softer than z_{cut}) affects **STD-D**

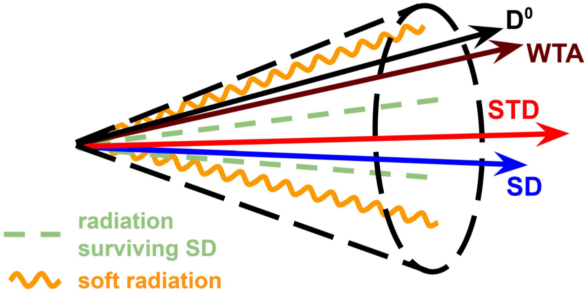

STD-SD shows how grooming changes the jet axis direction.

SD-D and **STD-SD** (z_{cut} varied, β=0)

$$\frac{min(p_{T_1}, p_{T_2})}{p_{T_1} + p_{T_2}} > z_{cut} \left(\frac{\Delta R_{12}}{R}\right)^{\beta}$$

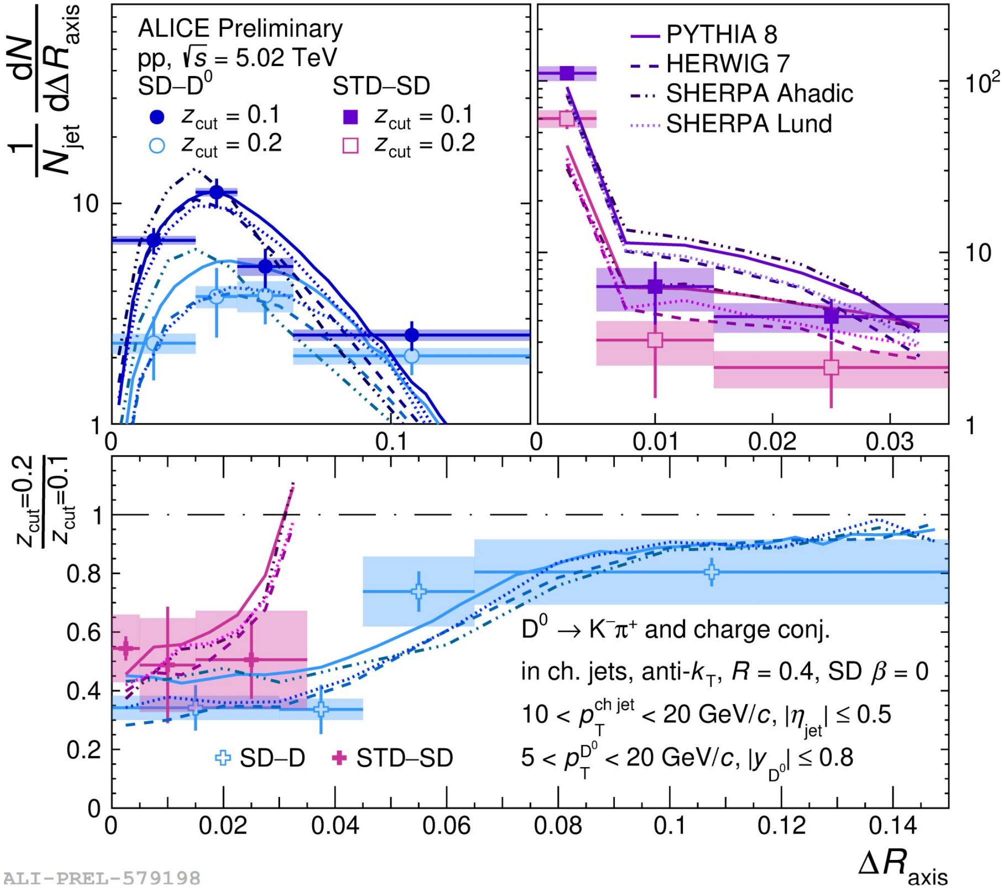

ALI-PREL-579198

There's a lot of information here, let's take it one panel at a time…

SD-D and **STD-SD** (z_{cut} varied, β=0)

$$\frac{min(p_{T_1}, p_{T_2})}{p_{T_1}+p_{T_2}} > z_{cut}\left(\frac{\Delta R_{12}}{R}\right)^{\beta}$$

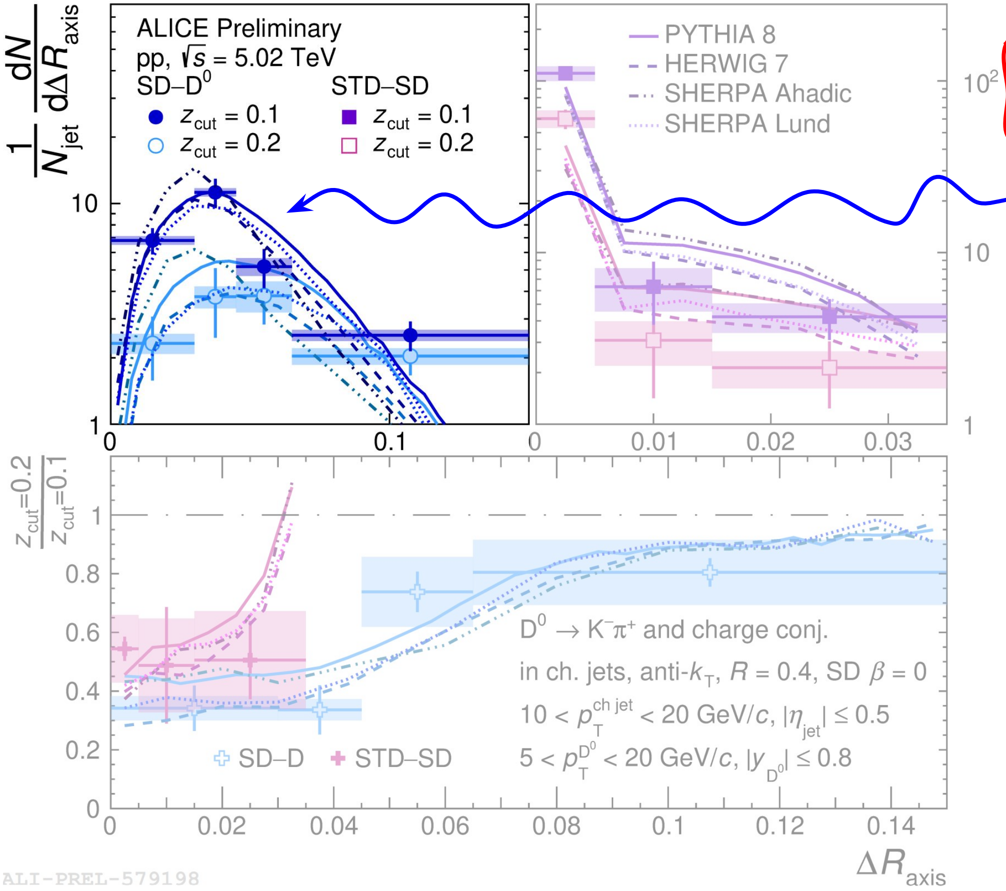

Remember **STD-D** peaked in the first bin of ΔR

…but for **SD-D (z_{cut}=0.1)**, the first bin is where we see the most grooming

This region contains jets with very soft splittings off the charm quark, or none at all - which do not significantly tilt the jet direction with respect to the D^0 direction

Intensifying the grooming to **SD-D (z_{cut}=0.2)** shows how drastically jets at small ΔR are removed, while at large ΔR the distributions match

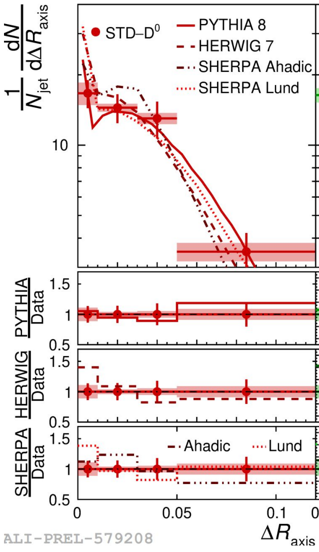

SD-D and **STD-SD** (z_{cut} varied, β=0)

$$\frac{min(p_{T_1},p_{T_2})}{p_{T_1}+p_{T_2}} > z_{cut}\left(\frac{\Delta R_{12}}{R}\right)^{\beta}$$

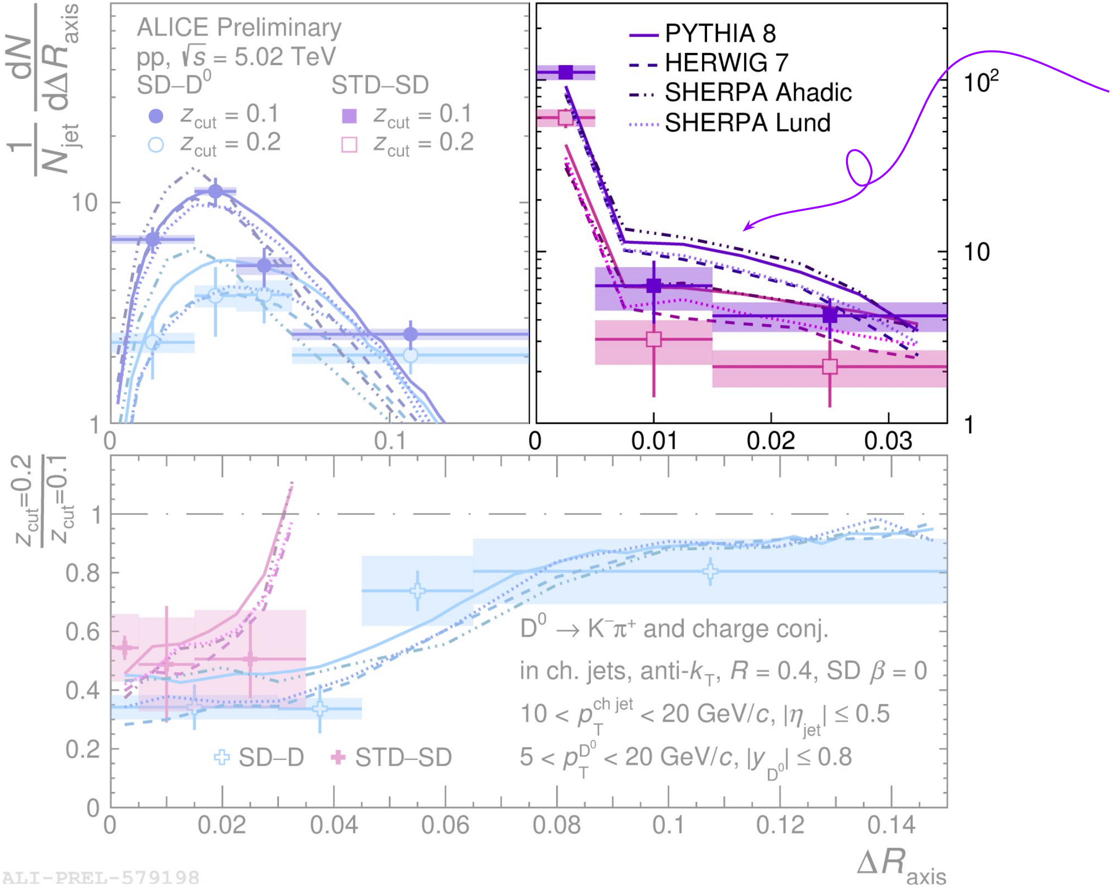

STD-SD shows how grooming changes the jet axis direction. The spike in the first bin includes jets where no branch gets groomed away (axes are aligned)

The shapes of **STD-SD (z_{cut}=0.1)** and **STD-SD (z_{cut}=0.2)** look very similar here… so we wanted to take a ratio of the two!

SD-D and **STD-SD** (z_{cut} varied, β=0)

$$\frac{min(p_{T_1}, p_{T_2})}{p_{T_1}+p_{T_2}} > z_{cut}\left(\frac{\Delta R_{12}}{R}\right)^{\beta}$$

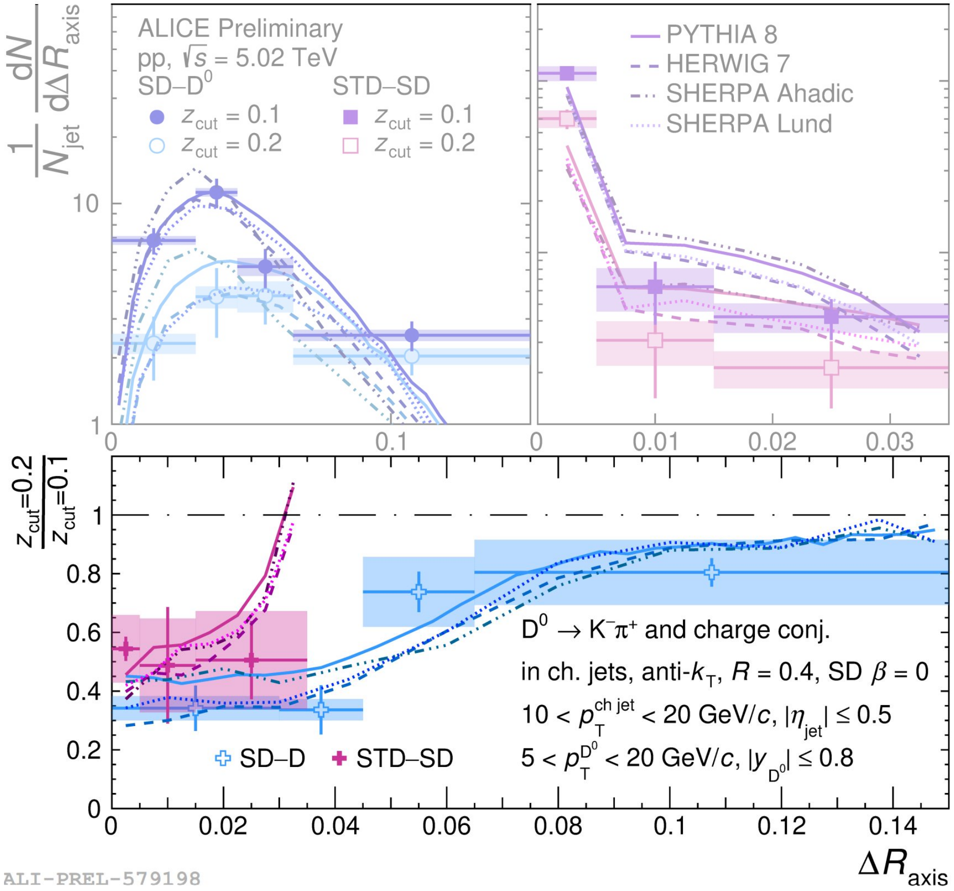

We took the ratio of **(z_{cut}=0.2)/(z_{cut}=0.1)** for both **SD-D** and **STD-SD**

- ➔ Grooming STD-SD removes half the total counts between z_{cut}=0.1 and z_{cut}=0.2
- ➔ Grooming SD-D affects small ΔR more than large ΔR

SD-D and **STD-SD** (z_{cut} varied, β=0)

$$\frac{min(p_{T_1}, p_{T_2})}{p_{T_1}+p_{T_2}} > z_{cut}\left(\frac{\Delta R_{12}}{R}\right)^{\beta}$$

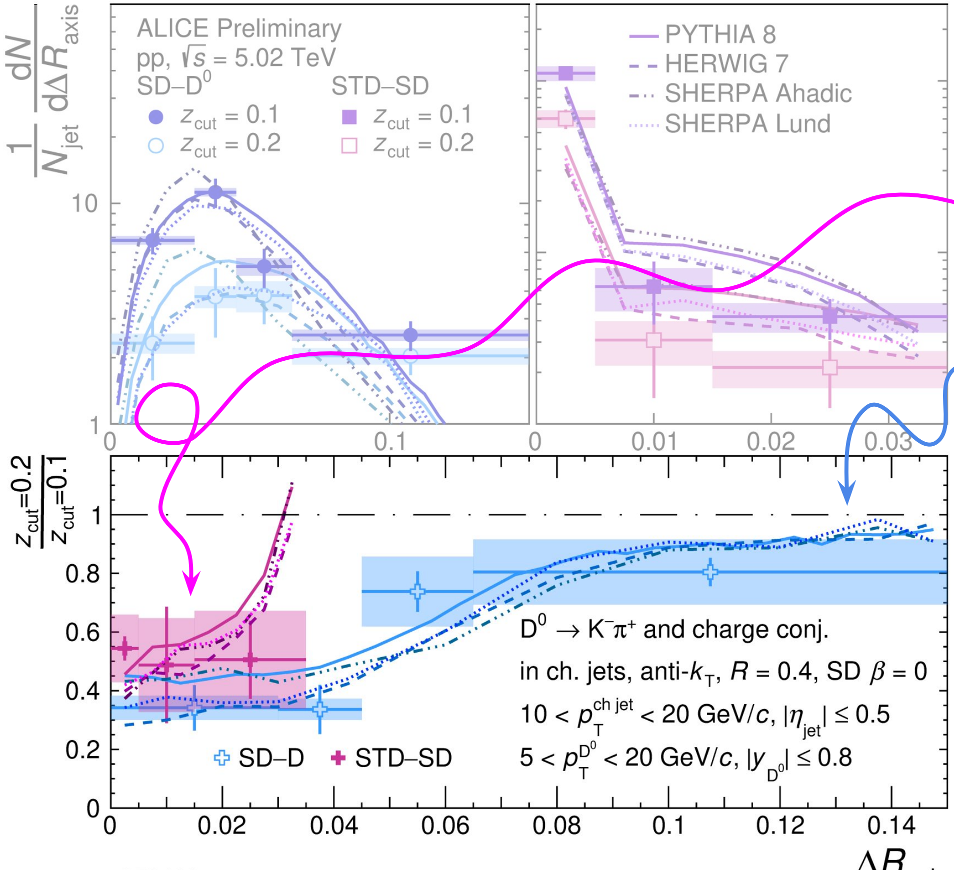

ALI-PREL-579198

We took the ratio of **(z_{cut}=0.1)/(z_{cut}=0.2)** for both **SD-D** and **STD-SD**

- Grooming STD-SD removes half the total counts between z_{cut}=0.1 and z_{cut}=0.2
- Grooming SD-D affects small ΔR more than large ΔR

Intensifying grooming from z_{cut}=0.1 to z_{cut}=0.2:

➔ …shows that radiation is removed uniformly with respect to the STD axis

➔ …shows that SD jets are more likely to survive grooming if the SD axis is further from the D^0

SD-D and STD-SD (z_{cut} varied, β=0)

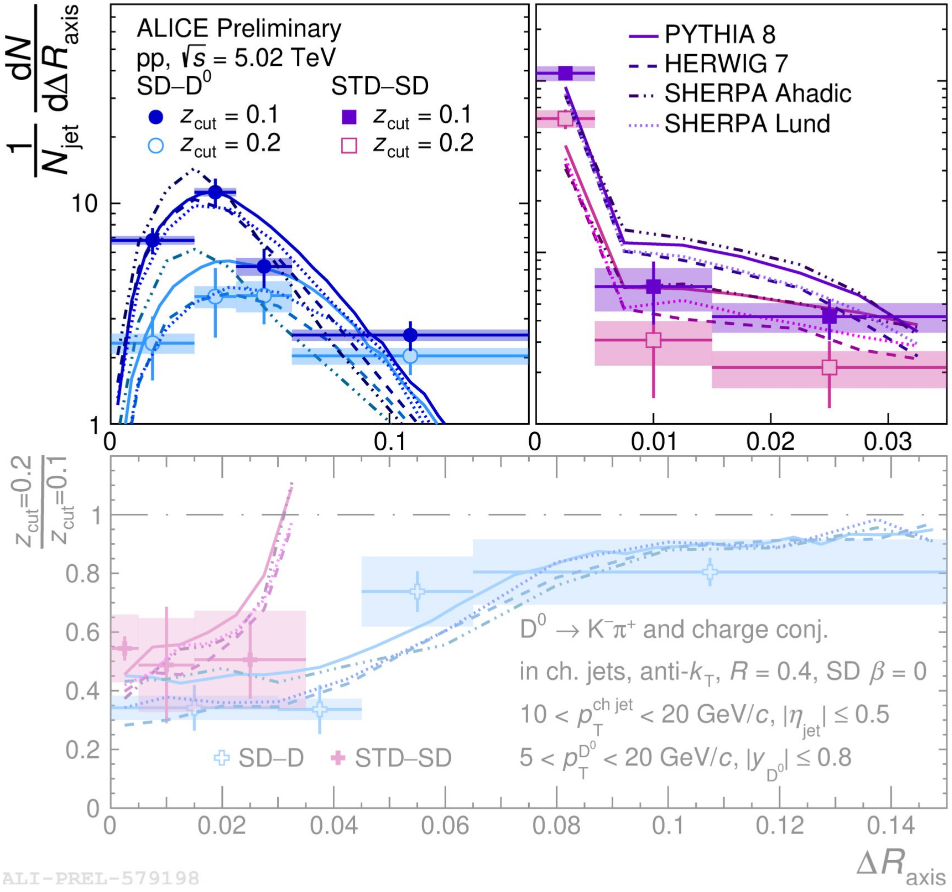

Comparison to Inclusive Jets

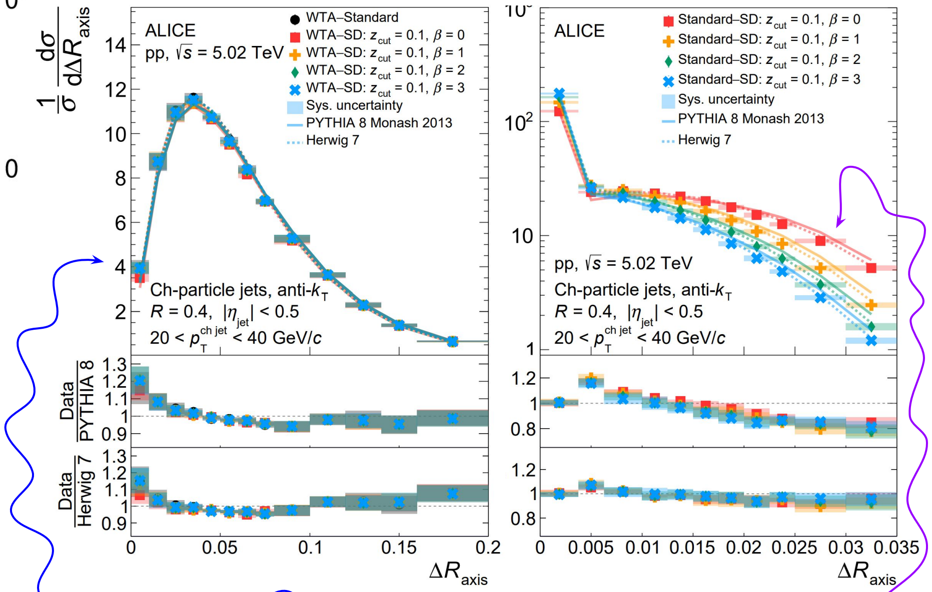

compare to
SD-D (z_{cut}=0.1)

compare to
STD-SD (z_{cut}=0.1)

SD-D and **STD-SD** (z_{cut} varied, β=0)

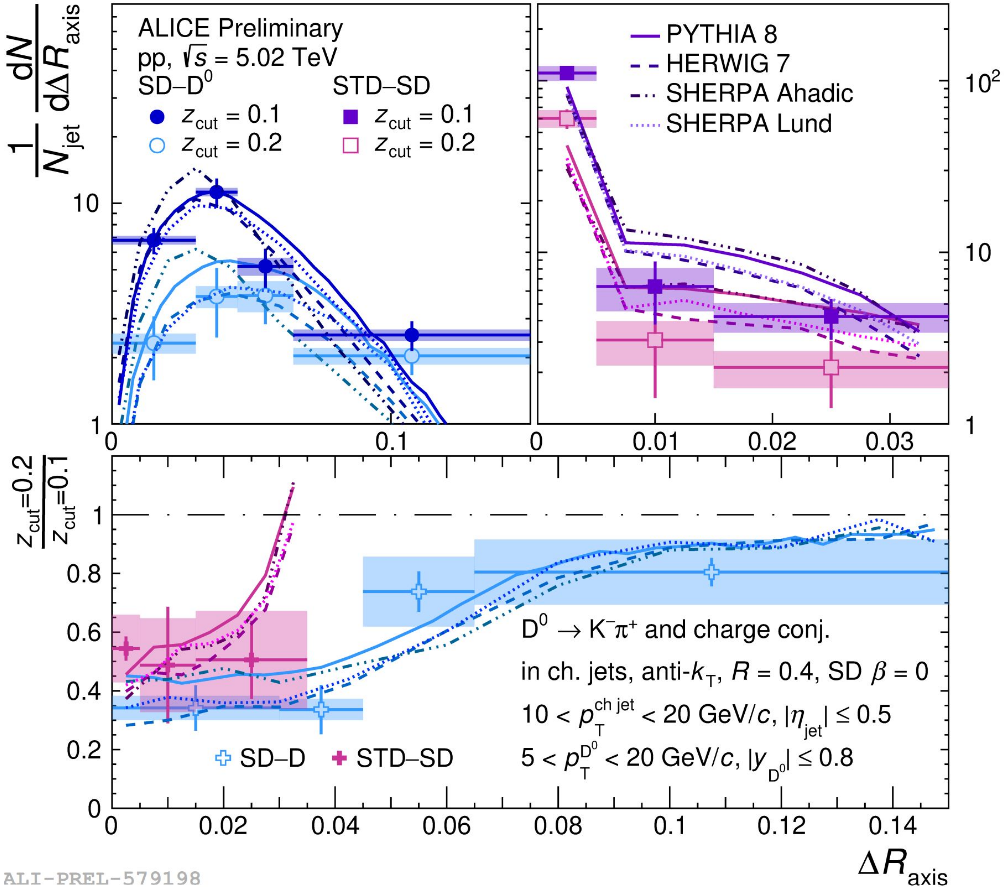

ALI-PREL-579198

Comparison to Generators

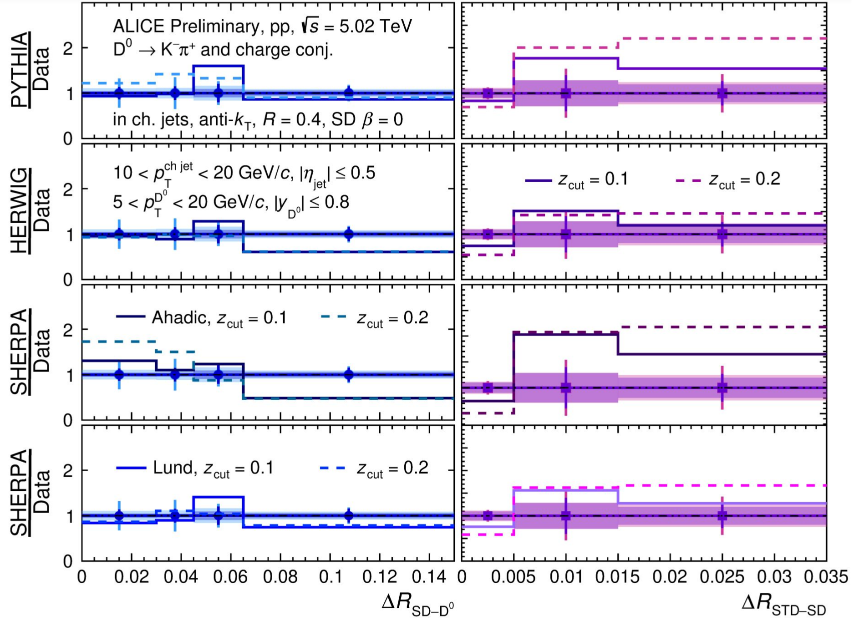

ALI-PREL-579203

SD-D and STD-SD (z_{cut} varied, β=0)

String-Based Generators: *PYTHIA and SHERPA Lund*
Cluster-Based Generators: *HERWIG and SHERPA Ahadic*

SD-D:

- String-based models match data, overall better predictions
- *HERWIG* predicts the least dependence on the z_{cut} parameter (also seen in inclusive)

STD-SD:

- String-based models describe the data better for z_{cut}=0.1 than z_{cut}=0.2
- *HERWIG* predicts the data best, less dependence on z_{cut} for large ΔR (also seen in inclusive)

HERWIG and *SHERPA Lund* provide best description of the groomed data.

Comparison to Generators

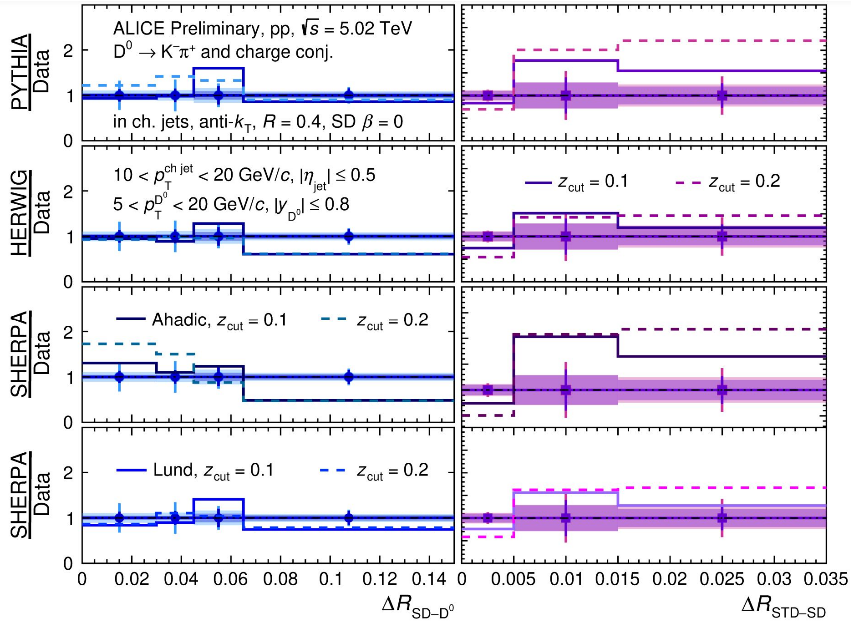

ALI-PREL-579203

Quick aside to another interesting ΔR result…

A comparison between D^0-tagged and Λ_c^+-tagged ΔR to access potential modifications of the hadronization of charm quarks

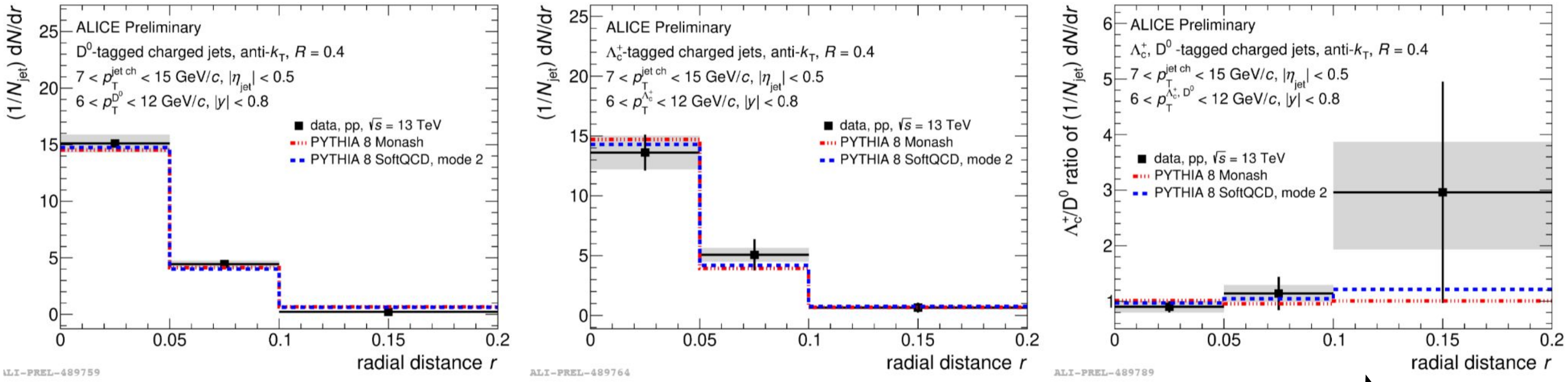

Are baryons less collimated than mesons with respect to the jet axis?
More statistics are needed! → Run 3 data is promising

Overview

UNIVERSITY OF
ILLINOIS
URBANA-CHAMPAIGN

Result #1: The D^0 does not necessarily define the Standard axis direction

Result #2: The standard jet sample is described best by *PYTHIA*

Result #3: In the given kinematic range, the D^0 is the leading particle in 99% of jets in 10-20 p_T^{jet}

ungroomed sample of jets

Result #4: Jets are more likely to survive intense grooming when the SD axis is further away from the D^0. In inclusive WTA-SD, grooming had minimal impact

Result #5: Radiation is removed uniformly in ΔR with respect to the STD axis

Result #6: *HERWIG* and *SHERPA Lund* describe the groomed data best. *HERWIG* has minimal zcut dependence - also seen in inclusive jets

groomed sample of jets

First D^0-tagged jet axes difference measurement ! A paper is on its way with interesting new content :)

Thank you for listening and for the opportunity to speak !

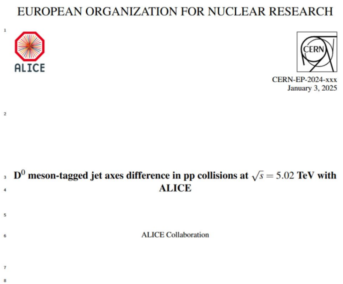

EUROPEAN ORGANIZATION FOR NUCLEAR RESEARCH

ALICE

CERN-EP-2024-xxx
January 3, 2025

D^0 meson-tagged jet axes difference in pp collisions at $\sqrt{s} = 5.02$ TeV with ALICE

ALICE Collaboration

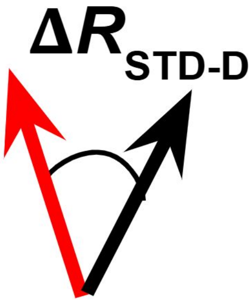

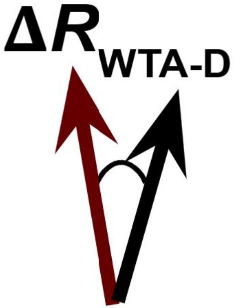

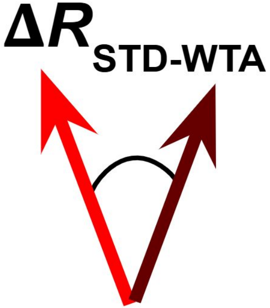

Backup Slides

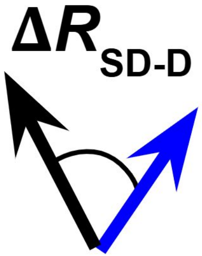

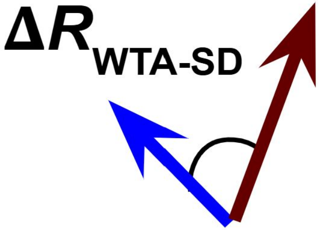

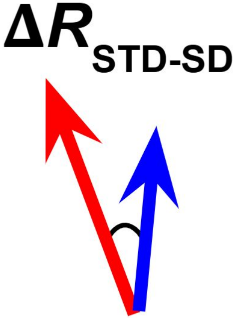

Final Plots *SD-D vs WTA-SD (zcut=0.1)*

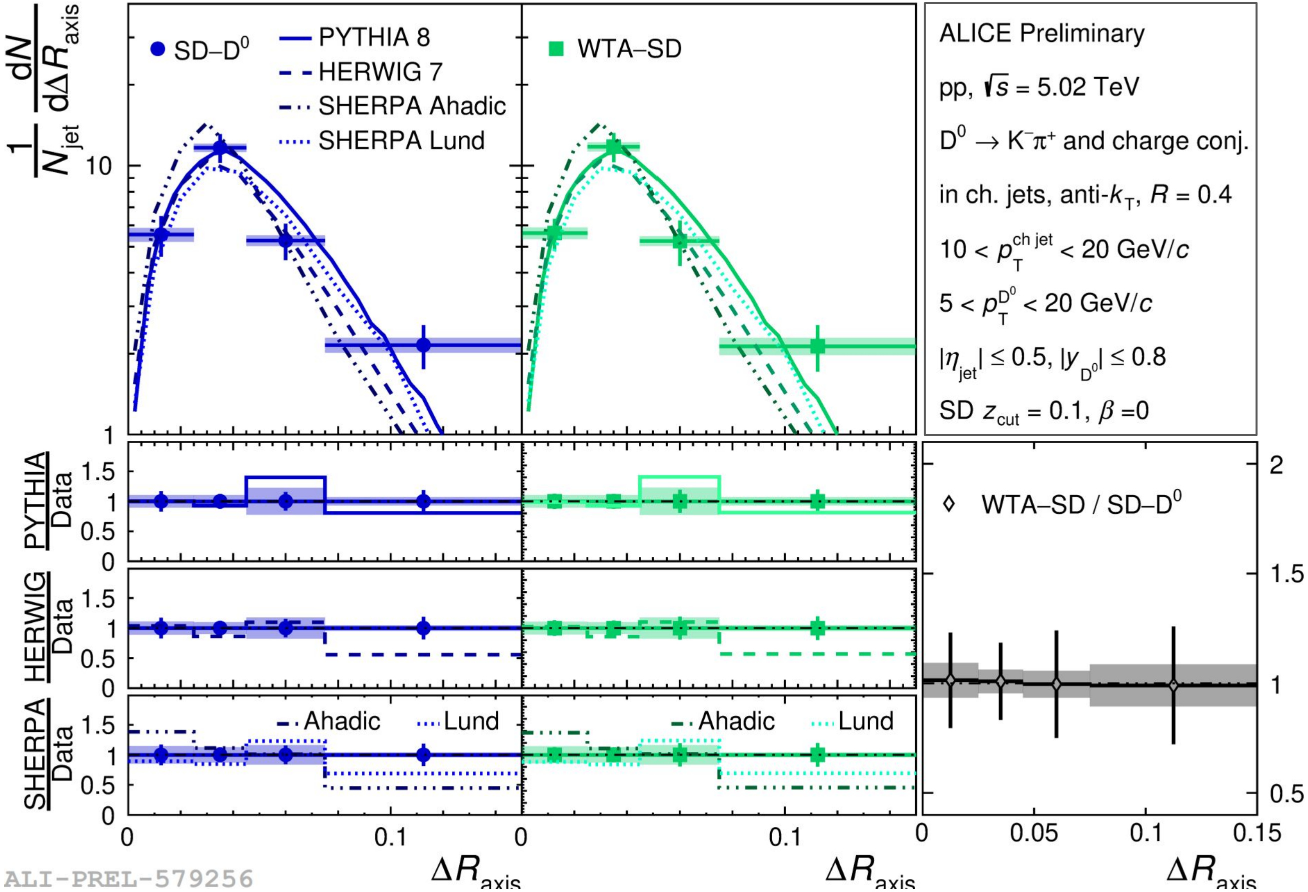

SD-D matches **WTA-SD**!
- ➔ p-value = 0.999995
- ➔ PYTHIA predicts the data less well

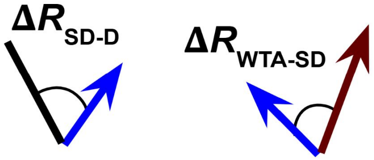

$$\frac{min(p_{T_1}, p_{T_2})}{p_{T_1} + p_{T_2}} > z_{cut} \left(\frac{\Delta R_{12}}{R}\right)^{\beta}$$

Comparison to Generators:
- ➔ String-based models match and have most accurate predictions
- ➔ Herwig also shows a flatter trend here, but Sherpa Ahadic hints at some shape dependency

Final Plots *SD-D vs WTA-SD (zcut=0.2)*

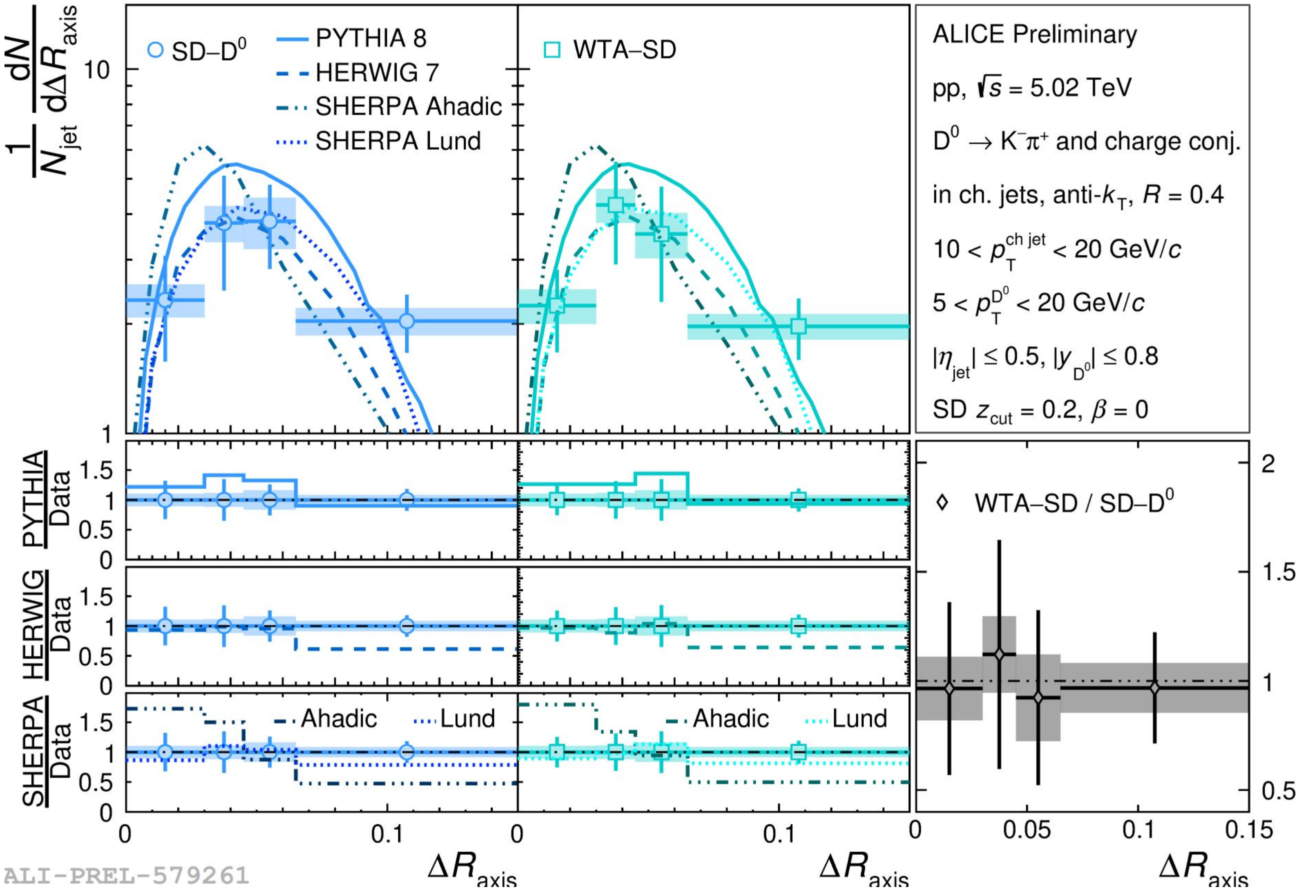

SD-D matches **WTA-SD**!
- ➔ p-value = 0.99887
- ➔ PYTHIA predicts the data fairly well

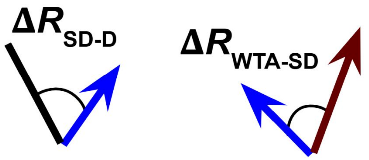

$$\frac{min(p_{T_1}, p_{T_2})}{p_{T_1} + p_{T_2}} > z_{cut}\left(\frac{\Delta R_{12}}{R}\right)^{\beta}$$

Comparison to Generators:
- ➔ String-based models match, slightly more accurate than zcut=0.1
- ➔ Cluster-based models look relatively unchanged from zcut=0.1 case - also seen for inclusive jets

Final Plots *STD-SD (zcut varied)*

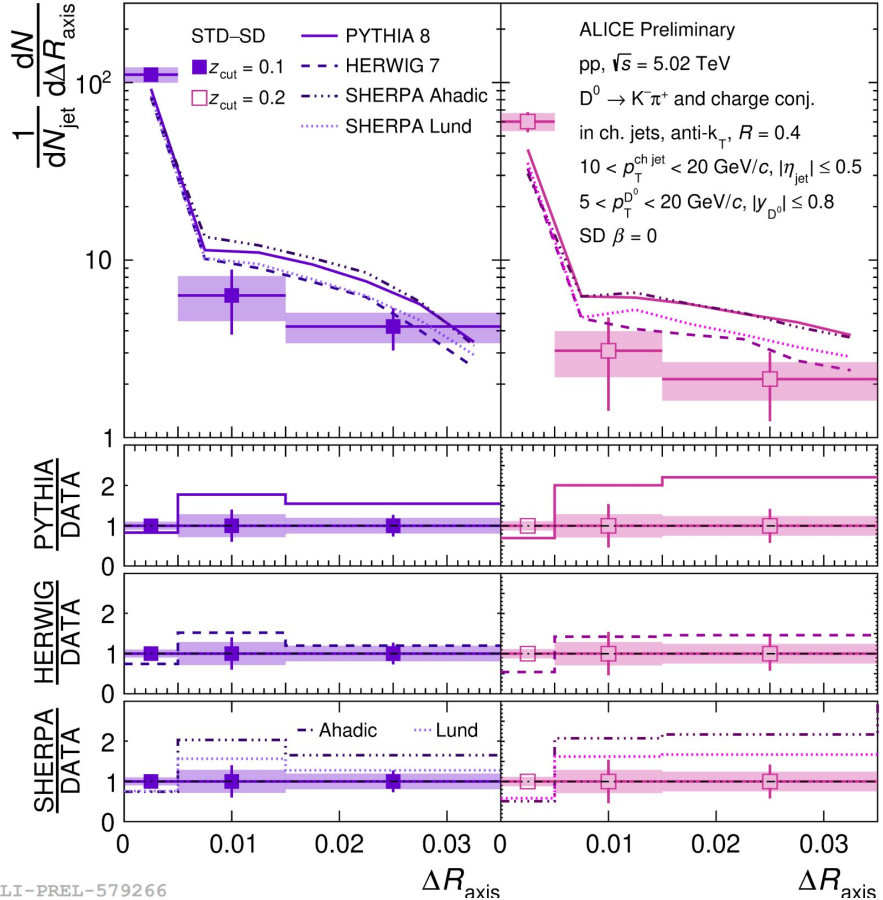

ALI-PREL-579266

- ➔ Grooming does not change the overall shape for **STD-SD.**
- ➔ More information on next slide…

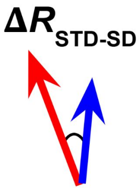

Comparison to Generators:

- ➔ Herwig predicts well and equivalently between values of zcut (also seen for inclusive case), while string-based models predict better for zcut=0.1 compared to 0.2
- ➔ Pythia looks more like Sherpa Ahadic here, and Herwig more like Sherpa Lund? But all similar shapes considering statistical errors

Analysis Methods: More Details

Signal Shape Extraction

Extracting the raw D^0 signal:

- ➔ Fitted the sideband shapes (B1 and B2) to an exponential function over the full range
- ➔ Fitted the signal (A) to a gaussian function over the full range

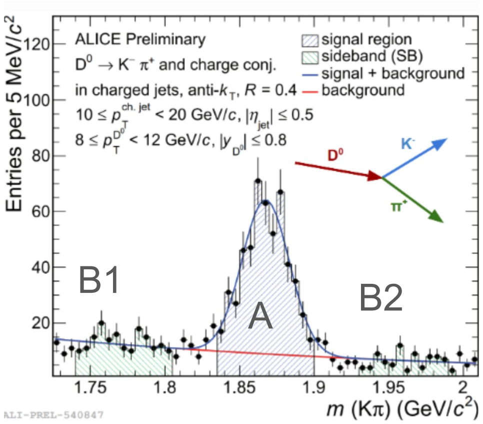

- ➔ Totalled the sideband shape distributions and subtracted that from the measured signal.

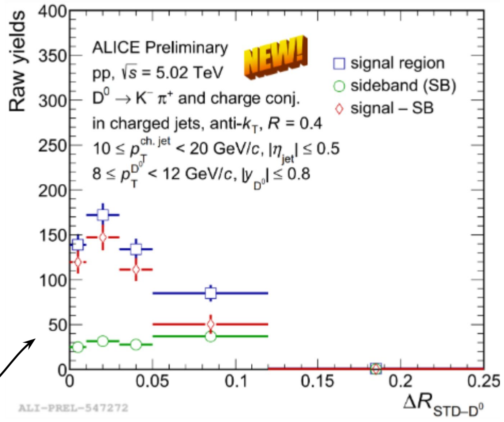

- ➔ We also remove reflection particles, which have swapped mass assignment, by generating a reflection-only sample in MC and subtracting that from the data signal.
  - ◆ Reflection contribution is largest at smaller pT

Analysis Methods: More Details

D^0 Reconstruction Efficiency Correction

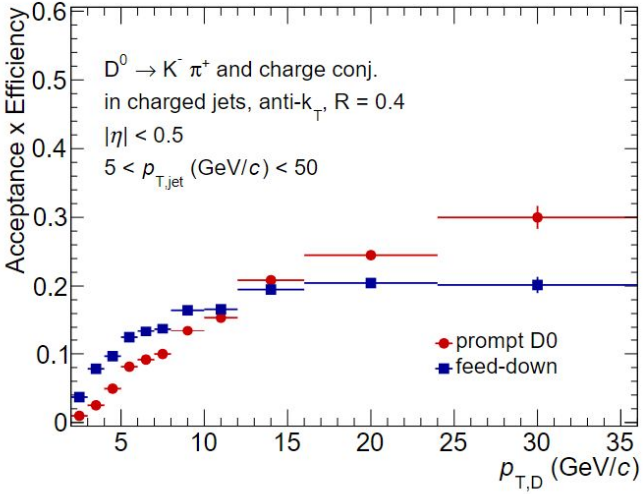

Measured signal needs to be corrected for D^0 reconstruction, topological and PID selection efficiencies

- ➔ Efficiency of the D^0 cut selections is strongly dependent on D^0-meson pT
  - ◆ The selections are stricter at low D^0 pT so that the larger combinatorial background can be removed

The sideband-subtracted distributions are corrected by the D^0 reconstruction and selection efficiency in each D^0 pT interval

The efficiency-corrected jet axes differences are then integrated over D^0 intervals

Analysis Methods: More Details

Beauty Decay Correction (non-prompt)

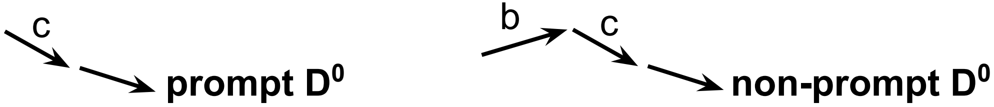

The non-prompt D^0 should be removed as it did not originate from the charm quark in the initial stages of the collisions.

- ➔ estimated with **POWHEG+PYTHIA8**
- ➔ corrected with luminosity, branching ratio and reconstruction efficiency
- ➔ the non-prompt D^0 shape was folded to detector-level using a 4D Response Matrix and then subtracted from the efficiency-corrected ΔR

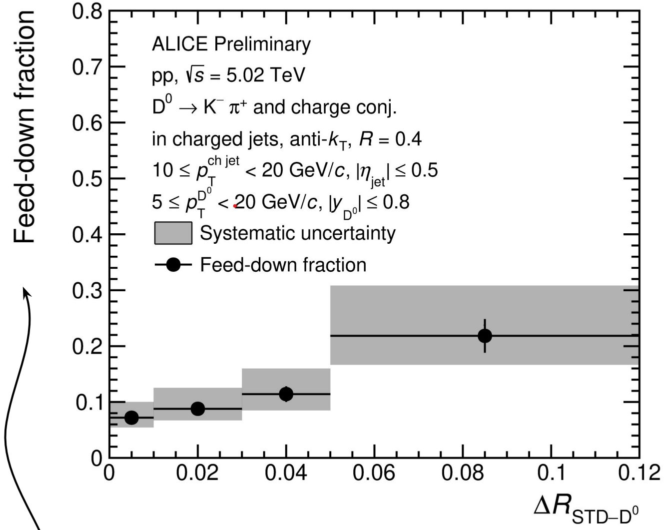

ALI-PREL-547264

$$= \frac{\text{non-prompt } \Delta R_{\rm D,jet}\ \textit{(Simulation)}}{\text{prompt+non-prompt } \Delta R_{\rm D,jet}\ \textit{(Data)}}$$

Analysis Methods: More Details

Correction for Detector Effects

The unfolding procedure accounts for track momentum resolution and tracking inefficiencies in the detector volume

uses 4-Dimensional Response Matrices to relate detector level (data) to truth level (simulation) information

- ➔ the feed-down distributions were **folded** to detector-level using the **non-prompt Response Matrix**
- ➔ after feed-down subtraction, the data were **unfolded** to truth-level using the **prompt 4D Response Matrix**

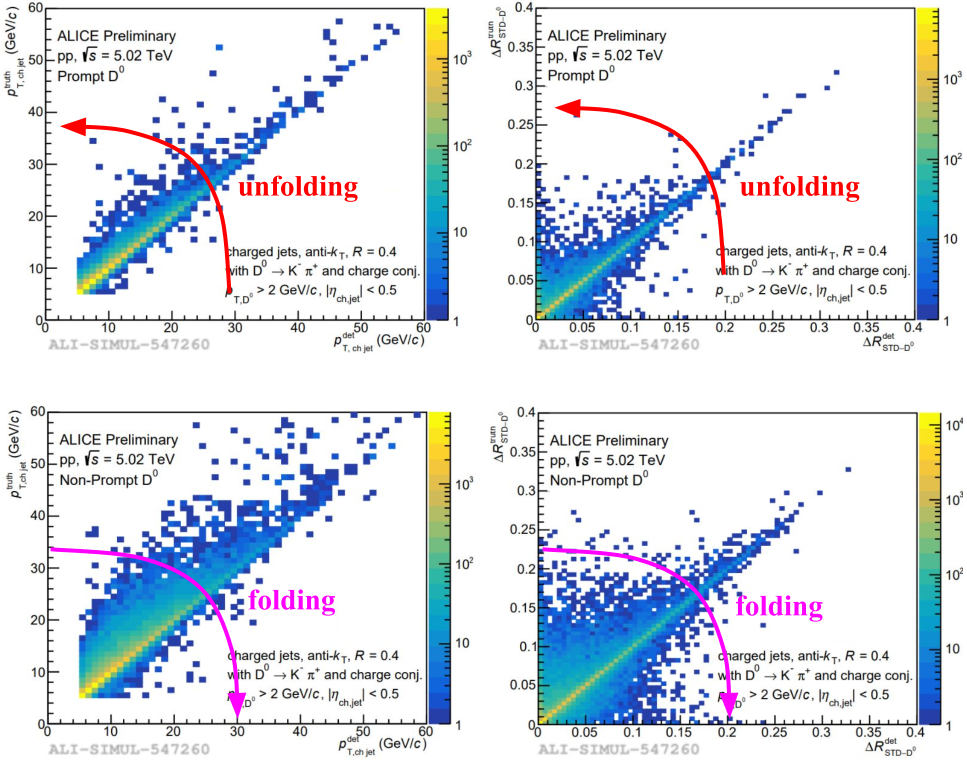

Comparison to Inclusive

STD-WTA

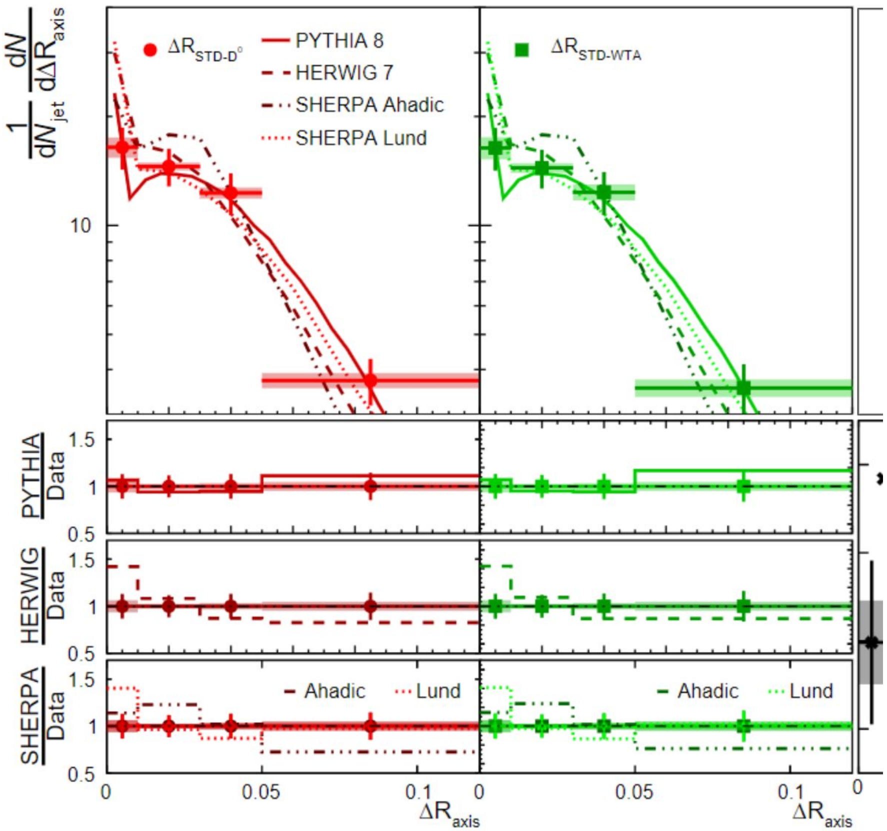

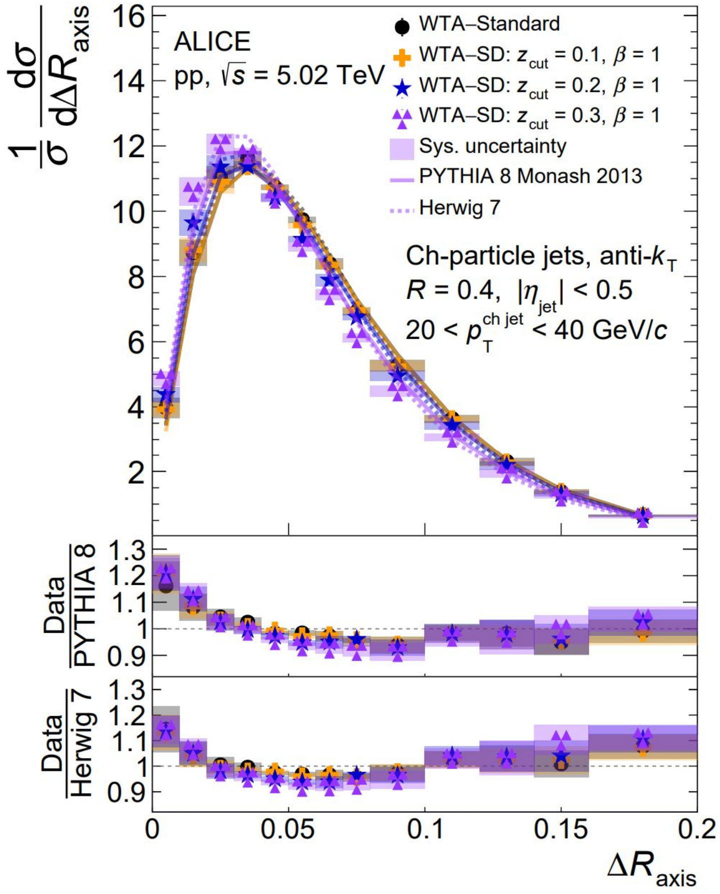

WTA-D Physics Message

$$z_{||}^{\mathrm{ch}} = \frac{\vec{p}_{\mathrm{ch\,jet}} \cdot \vec{p}_{\mathrm{D}^0}}{\vec{p}_{\mathrm{ch\,jet}} \cdot \vec{p}_{\mathrm{ch\,jet}}}$$

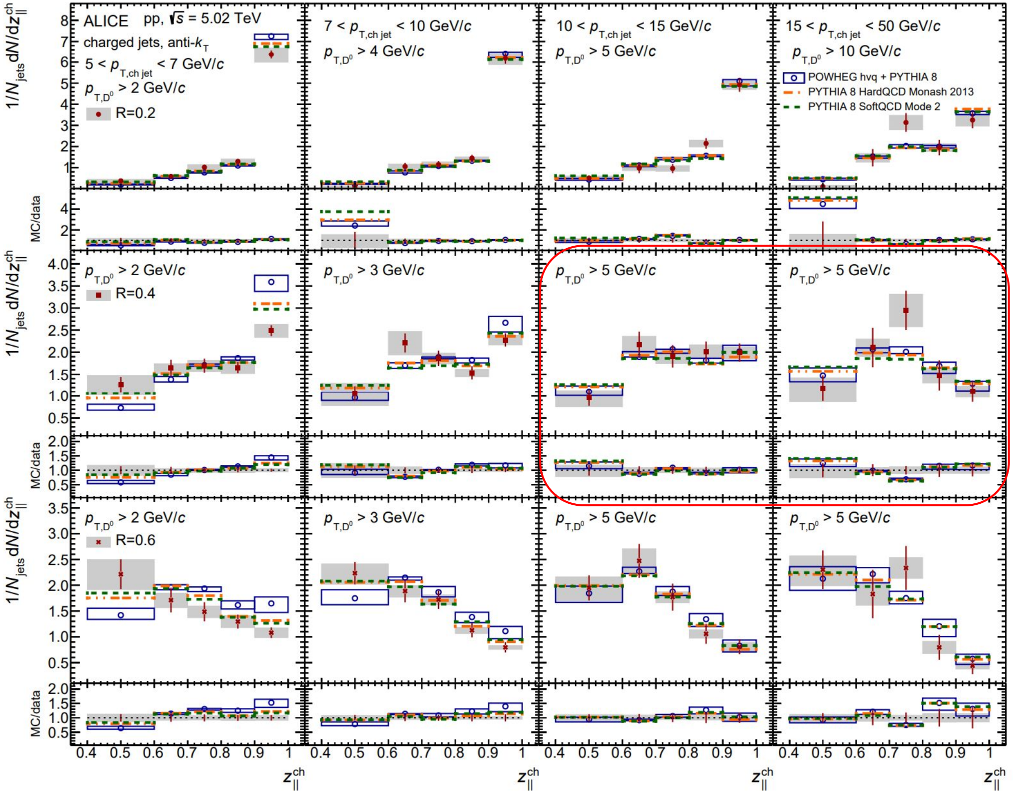

← This plot, from…

Measurement of the production of charm jets tagged with D0 mesons in pp collisions at √ s = 5.02 and 13 TeV

…is a study of momentum fraction carried by the D0 along the jet axis direction.

Studies of momentum fraction in 5.02TeV shows that for R=0.2 jets, the D0 carries most of the momentum. For R=0.4 jets the fragmentation starts to soften, but still concentrated above $z_{||}$=0.5.

- Softening is due to more fragments in the jet carrying away momentum.

WTA-D0 tells us that the D0 is in the hardest prong.

- Previous studies of the fragmentation of charm jets showed that the D0 is usually the leading particle, but WTA-D clearly shows **how often** the D0 is the winner (99% of the time).

https://arxiv.org/pdf/2204.10167

Analysis Methods: Systematic Ingredients

Tracking Efficiency: Randomly rejected 3% of tracks to account for uncertainty in the tracking for the dataset. RMS of the ratio of variation over default taken as an uncertainty.

Feed-down (non-prompt) Variation: Feeddown simulation performed with different choices of b-quark mass, factorization scale factor, renormalization scale factor and pdf choice. Maximum spread of the ratio taken as an uncertainty.

Yield Extraction: Standard variation of the signal extraction parameters for D0 jets, RMS of the ratio was calculated as an uncertainty. Varied the mean of the gaussian fit, background fitting functions, fitting range, rebinning, and the band-width variation.

Topological Cut Variations: Five standard variations of the selection criteria (±10%, ±20% deviations in the efficiency and one with an additional variation on the *topomatic cut* - the difference between the reconstructed and expected impact parameter value)

Unfolding: Standard deviation of the variations below taken as total uncertainty.

$$(p_{\mathrm{T}}^{\mathrm{ch\,jet}})^{\pm 0.5} \times (1 \pm 0.5 * (2\Delta R - 1))$$

- ➔ varied the regularization parameter (+/-2 units)
- ➔ varied the prior by the equation shown. Maximum of the variation chosen for each bin as the uncertainty.
- ➔ varied the truncation of the detector-level jet pT (by 1 GeV/c).
- ➔ Unfolded alternate binning configurations by increasing and decreasing the size of each bin by at least 20% of its original size. We then took a linear fit of the ratio of the variations over the default as a systematic.

Analysis Methods: Systematics

Summary Table

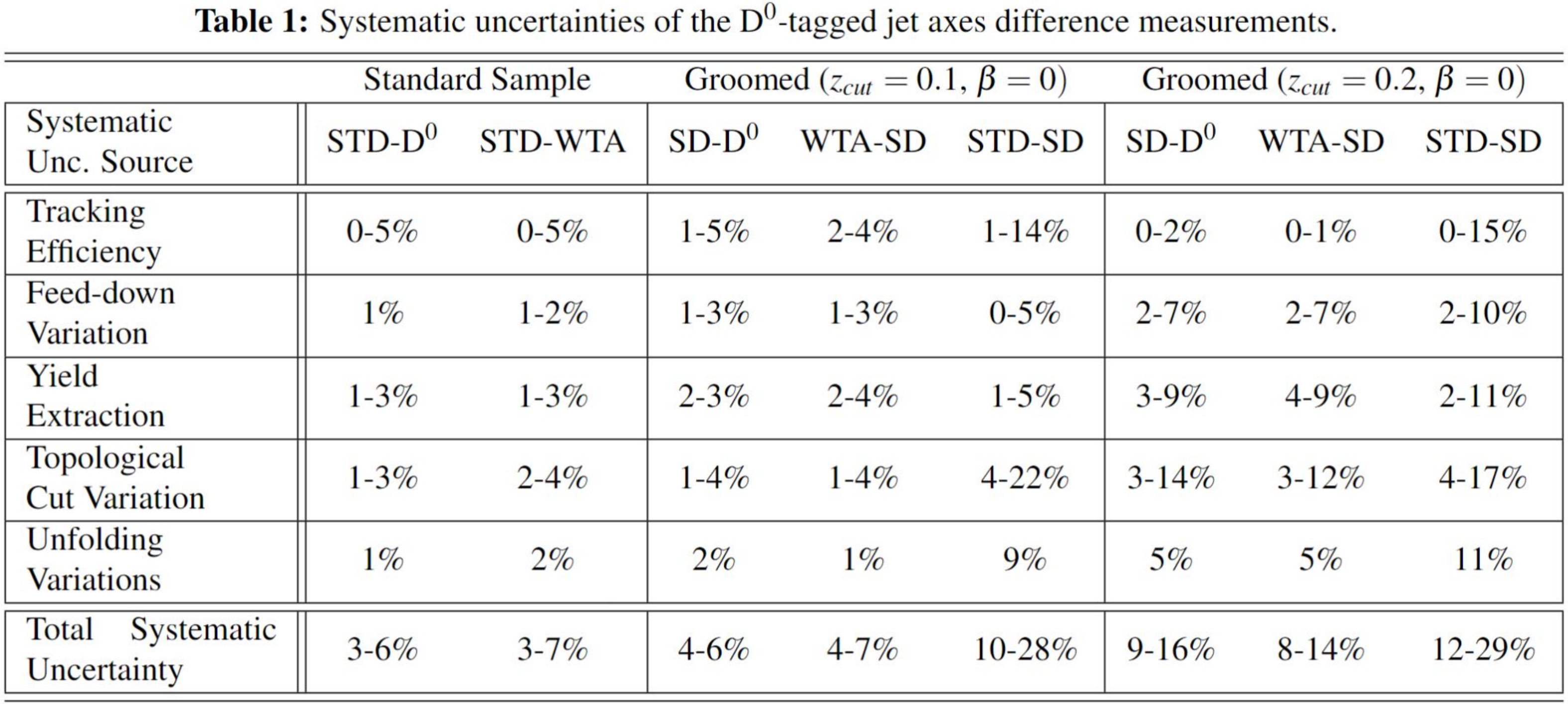

Table 1: Systematic uncertainties of the D^0-tagged jet axes difference measurements.

	Standard Sample		Groomed ($z_{cut} = 0.1, \beta = 0$)			Groomed ($z_{cut} = 0.2, \beta = 0$)		
Systematic Unc. Source	STD-D^0	STD-WTA	SD-D^0	WTA-SD	STD-SD	SD-D^0	WTA-SD	STD-SD
Tracking Efficiency	0-5%	0-5%	1-5%	2-4%	1-14%	0-2%	0-1%	0-15%
Feed-down Variation	1%	1-2%	1-3%	1-3%	0-5%	2-7%	2-7%	2-10%
Yield Extraction	1-3%	1-3%	2-3%	2-4%	1-5%	3-9%	4-9%	2-11%
Topological Cut Variation	1-3%	2-4%	1-4%	1-4%	4-22%	3-14%	3-12%	4-17%
Unfolding Variations	1%	2%	2%	1%	9%	5%	5%	11%
Total Systematic Uncertainty	3-6%	3-7%	4-6%	4-7%	10-28%	9-16%	8-14%	12-29%

Jet Algorithms

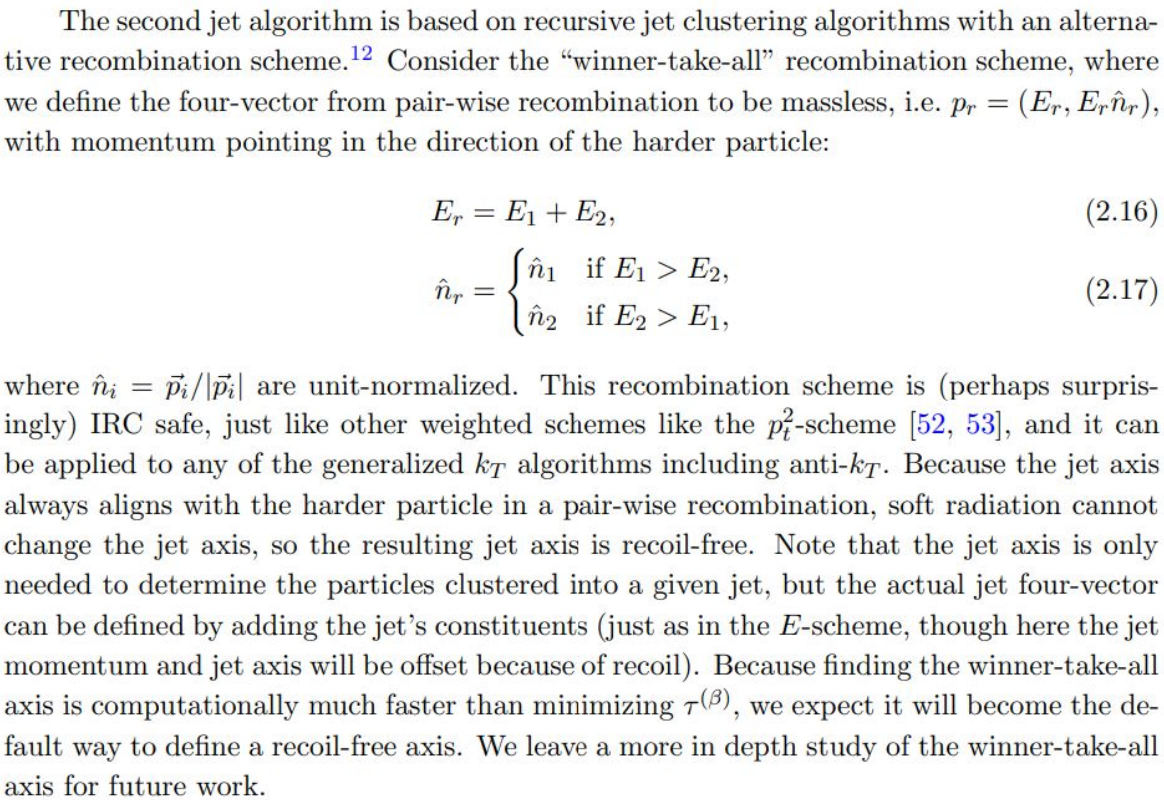

The second jet algorithm is based on recursive jet clustering algorithms with an alternative recombination scheme.[12] Consider the "winner-take-all" recombination scheme, where we define the four-vector from pair-wise recombination to be massless, i.e. $p_r = (E_r, E_r \hat{n}_r)$, with momentum pointing in the direction of the harder particle:

$$E_r = E_1 + E_2, \tag{2.16}$$

$$\hat{n}_r = \begin{cases} \hat{n}_1 & \text{if } E_1 > E_2, \\ \hat{n}_2 & \text{if } E_2 > E_1, \end{cases} \tag{2.17}$$

where $\hat{n}_i = \vec{p}_i/|\vec{p}_i|$ are unit-normalized. This recombination scheme is (perhaps surprisingly) IRC safe, just like other weighted schemes like the p_t^2-scheme [52, 53], and it can be applied to any of the generalized k_T algorithms including anti-k_T. Because the jet axis always aligns with the harder particle in a pair-wise recombination, soft radiation cannot change the jet axis, so the resulting jet axis is recoil-free. Note that the jet axis is only needed to determine the particles clustered into a given jet, but the actual jet four-vector can be defined by adding the jet's constituents (just as in the E-scheme, though here the jet momentum and jet axis will be offset because of recoil). Because finding the winner-take-all axis is computationally much faster than minimizing $\tau^{(\beta)}$, we expect it will become the default way to define a recoil-free axis. We leave a more in depth study of the winner-take-all axis for future work.

Winner-Take-All axis
Reclustered with C-A algorithm and recombination with Winner-Take-All scheme

- **WTA scheme:** At each recombination step, the resulting prong has the direction of the hardest sub-prong and a p_T equal to the sum of the two sub-prongs p_T.

Groomed axis
Groom jet with the Soft Drop (SD) algorithm.

$$\frac{min(p_{T_1}, p_{T_2})}{p_{T_1} + p_{T_2}} > z_{cut}\left(\frac{\Delta R_{12}}{R}\right)^{\beta}$$

Less sensitive to soft radiation than standard

PYTHIA Studies

Momentum Fraction, $z = p_{T,\,D0} / p_{T,\,jet}$

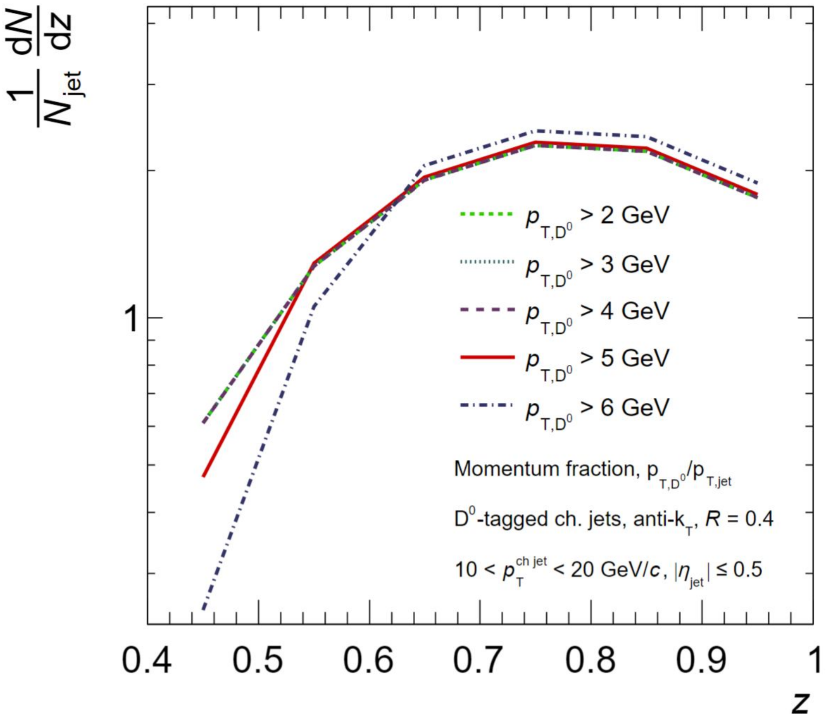

$p_{T,\,D0}$ threshold	$\frac{0.4 < z < 0.5}{0 < z < 1}$	$\frac{0 < z < 0.5}{0 < z < 1}$
$p_{T,\,D0} > 2$ GeV	0.059516	0.0830808
$p_{T,\,D0} > 3$ GeV	0.0596169	0.080897
$p_{T,\,D0} > 4$ GeV	0.0600098	0.0742316
$p_{T,\,D0} > 5$ GeV	0.0469394	0.0530865
$p_{T,\,D0} > 6$ GeV	0.0251881	0.027616

- For our kinematic range, roughly 5% of our D0-mesons have z<1/2
- Pythia does not predict an extremely strong dependence on the $p_{T,\,D0}$ threshold

PYTHIA Studies

Momentum Fraction, $z = p_{T,\,D0} / p_{T,\,jet}$

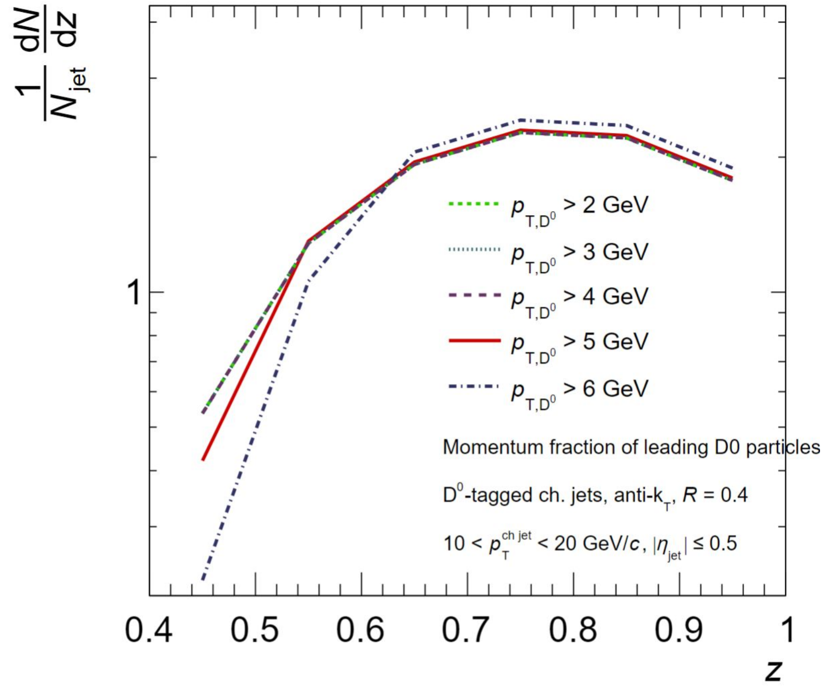

$p_{T,\,D0}$ threshold	$\frac{0.4 < z < 0.5}{0 < z < 1}$	$\frac{0 < z < 0.5}{0 < z < 1}$
$p_{T,\,D0} > 2$ GeV	0.0530054	0.0661984
$p_{T,\,D0} > 3$ GeV	0.0529751	0.0659669
$p_{T,\,D0} > 4$ GeV	0.0531323	0.0624714
$p_{T,\,D0} > 5$ GeV	0.0419208	0.0460682
$p_{T,\,D0} > 6$ GeV	0.0227434	0.0244747

- For our kinematic range, 4.6% of our D0-mesons that are leading have z<1/2
- Together with the previous slide, 5.3%-4.6% = 0.7% of D0's that are NOT the leading particle, according to these D0 momentum fraction pythia studies

PYTHIA Studies

Momentum Fraction, $z = p_{T,\,D0} / p_{T,\,jet}$

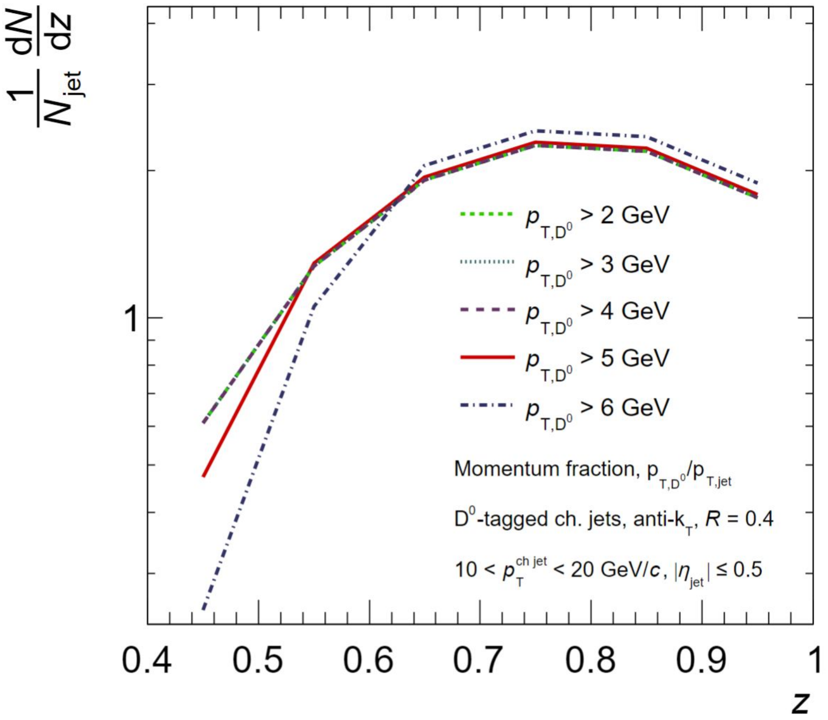

$p_{T,\,D0}$ threshold	$\frac{\text{D0 = leading particle}}{\text{All jets}}$
$p_{T,\,D0} > 2$ GeV	0.981884
$p_{T,\,D0} > 3$ GeV	0.983979
$p_{T,\,D0} > 4$ GeV	0.987419
$p_{T,\,D0} > 5$ GeV	0.992606
$p_{T,\,D0} > 6$ GeV	0.996771

- For our kinematic range, WTA-D are aligned 99% of the time with a 1% systematic uncertainty.
- Pythia does not predict an extremely strong dependence on the $p_{T,\,D0}$ threshold